MOLECULAR AND CELLULAR BIOLOGY, Aug. 2008, p. 5120–5138 Vol. 28, No. 16
0270-7306/08/$08.00+0 doi:10.1128/MCB.00786-08

Role of Nucleotide Binding in Septin-Septin Interactions and Septin Localization in *Saccharomyces cerevisiae*▽†

Satish Nagaraj,[1]‡ Ashok Rajendran,[1,2] Charles E. Jackson,[2] and Mark S. Longtine[1,2]*

Department of Biochemistry and Molecular Biology, Oklahoma State University, Stillwater, Oklahoma,[1] and Department of Cell Biology and Physiology, Washington University School of Medicine, St. Louis, Missouri[2]

Received 15 May 2008/Accepted 21 May 2008

Septins are a conserved family of eukaryotic GTP-binding, filament-forming proteins. In *Saccharomyces cerevisiae*, five septins (Cdc3p, Cdc10p, Cdc11p, Cdc12p, and Shs1p) form a complex and colocalize to the incipient bud site and as a collar of filaments at the neck of budded cells. Septins serve as a scaffold to localize septin-associated proteins involved in diverse processes and as a barrier to diffusion of membrane-associated proteins. Little is known about the role of nucleotide binding in septin function. Here, we show that Cdc3p, Cdc10p, Cdc11p, and Cdc12p all bind GTP and that P-loop and G4 motif mutations affect nucleotide binding and result in temperature-sensitive defects in septin localization and function. Two-hybrid, in vitro, and in vivo analyses show that for all four septins nucleotide binding is important in septin-septin interactions and complex formation. In the absence of complete complexes, septins do not localize to the cortex, suggesting septin localization factors interact only with complete complexes. When both complete and partial complexes are present, septins localize to the cortex but do not form a collar, perhaps because of an inability to form filaments. We find no evidence that nucleotide binding is specifically involved in the interaction of septins with septin-associated proteins.

Septins are a family of eukaryotic cytoskeletal proteins that assemble into hetero-oligomeric complexes and filaments (reviewed in references 27, 32, 44, 48, 54, 55, and 72). Septins were originally identified by temperature-sensitive lethal mutations in the *Saccharomyces cerevisiae CDC3*, *CDC10*, *CDC11*, and *CDC12* *c*ell *d*ivision *c*ycle (*CDC*) genes that resulted in elongated buds and an inability to undergo cytokinesis at restrictive temperature (36). In *S. cerevisiae*, septins are also involved in secretion, bud site selection, chitin deposition, response to mating pheromone, and in cell cycle checkpoints that respond to defects in morphogenesis, spindle orientation, and DNA damage (25, 71; reviewed in reference 55). In higher eukaryotes, septins are involved in cytokinesis, secretion, and the response to DNA damage and are functionally and physically interconnected with the actin and tubulin cytoskeletons. Septin defects have been implicated in several diseases, including infertility, Parkinson's disease, cancer, and others (29, 39, 51, 52; reviewed in references 27, 48, and 72).

During mitotic growth, *S. cerevisiae* expresses five septins: Cdc3p, Cdc10p, Cdc11p, Cdc12p, and Shs1p. Cdc3p, Cdc10p, Cdc11p, and Cdc12p are required for normal viability and are codependent for localization to the mother-bud neck, and the lack of any one of these septins inhibits or prevents the formation of septin filaments (22, 74). Shs1p is not essential for viability, the localization of the other septins, or for the formation of robust filaments and may have a specific role in localizing a subset of proteins of the actomyosin contractile ring (40, 74). About 10 min prior to bud emergence, the Cdc42p small GTPase directs septins to the cell cortex at the presumptive bud site by a pathway that involves direct interactions of septins with Gic1p and Gic2p, a related pair of Cdc42p effector proteins, and by a redundant, poorly characterized pathway (41, 45). The septins then assemble into a cortical ring and expand during bud emergence to form a cortical collar at the mother-bud neck composed of filaments that are oriented along the long axis of the cell (77). Cdc42p-GTP appears sufficient for localization of septins to the cortex, but Cdc42p-GTP hydrolysis may be required for release of septins from cortical localization factors or the assembly of septin filaments (11, 26). Upon activation of the mitotic exit network, the septin collar reorganizes into two rings with a coincident (and remarkable) 90° reorientation of the filaments (77). Actomyosin ring contraction and septum formation occur between the divided rings. Changes in septin organization are correlated with changes in dynamics: septins in rings in unbudded cells and following collar splitting are highly dynamic, undergoing rapid subunit exchange, while subunit exchange is slow in the septin collar (55), presumably because these septins are organized into higher-order structures.

Cortical septins at the mother-bud neck have multiple functions, including serving as a scaffold for the recruitment of septin-associated proteins to the neck, providing spatial and temporal regulation to their site of function (reviewed in references 28 and 55). Interactions with septins may also regulate the activity of septin-associated proteins (5, 33, 43, 50). The septin collar acts as a barrier to the movement of membrane-associated proteins involved in cell cycle progression and polarized growth (55). Late in the cell cycle, the divided septin

* Corresponding author. Mailing address: Department of Cell Biology and Physiology, Washington University School of Medicine, Campus Box 8228, 660 S. Euclid Ave., St. Louis, MO 63110. Phone: (314) 362-4606. Fax: (314) 362-7463. E-mail: mark.longtine@cellbiology.wustl.edu.

† Supplemental material for this article may be found at http://mcb.asm.org/.

‡ Current address: The Samuel Roberts Noble Foundation, Ardmore, OK.

▽ Published ahead of print on 9 June 2008.

rings are required for the retention to the mother-bud neck of cortical proteins involved in cytokinesis and septum formation (17).

Septins have a variable-length N-terminal region that typically contains a polybasic motif that may be involved in phospholipid binding and a C-terminal region that typically contains a predicted coiled-coil (reviewed in reference 63). The central G domain contains P-loop, G3, and G4 motifs that are present in many proteins that bind guanine nucleotides (63, 70). The recent solution of the structure of mammalian Sept2, Sept6, and Sept7 complexes bound to nucleotide revealed the septin G domain consists of six β-strands and five α-helices that are colinear with analogous regions of secondary structure in small GTPases, such as Ras, and that the septin G domain folds into a tertiary structure similar to that of canonical GTPases with the P-loop, G3, and G4 motifs positioned around the nucleotide. Septins also contain several unique α-helices and β-strands, and septins assemble into hetero-oligomeric complexes by interactions of the G domains and septin-unique structures. Linear asymmetric subcomplexes containing one of each type of septin associate head-to-head, forming an apolar core complex with two of each septin. Tail-to-tail associations result in apolar filaments, with filament pairing and bundling apparently mediated by interactions between the coiled-coil regions extending from the filament (42, 70). However, despite their conservation, the roles of complexes and filaments in septin function are not understood.

Septin complexes copurify with stoichiometric amounts of guanine nucleotides, typically with an ~2.1:2.4 ratio of GTP:GDP, and many septins bind and hydrolyze GTP in vitro. However, as not all septins are able to detectably bind GTP after individual expression in *Escherichia coli* (75), it is possible that nucleotide binding is not a universal property of septins.

A major outstanding issue is the role of nucleotide binding and hydrolysis in septin function. One model is that septins undergo multiple rounds of GTP binding and hydrolysis and that the changes in the status of the bound nucleotide regulate the assembly or disassembly of filaments, as occurs with β-tubulin, or the assembly and disassembly of septin complexes. This seems unlikely, as yeast septins bind and hydrolyze only a single nucleotide per protein lifetime (76), both GDP- and GTP-bound septins assemble into complexes and filaments, and the exogenous addition of GTP to hetero-oligomeric septin complexes does not enhance filament assembly (21, 49, 69, 70, 76). Another model is that GTP binding or hydrolysis may regulate interactions of septins with septin-associated proteins, thereby regulating their function, as has been suggested for septins interacting with the syntaxin SNARE and the GLAST glutamate transporter (6, 50). However, that septin function is regulated in this manner in vivo has not been demonstrated. A third model is that nucleotide binding by septins may have a structural role, similar to that of nucleotide binding by α-tubulin. Finally, a recent study suggested that nucleotide binding has a specific role in the assembly of complexes into filaments (75).

In this study, we have investigated the role of nucleotide binding in the function of Cdc3p, Cdc10p, Cdc11p, and Cdc12p. We conclude that all four septins bind guanine nucleotides and that nucleotide binding is important in septin-septin interactions and septin complex formation. Septin localization is perturbed in mutants with altered complexes, indicating a requirement for complexes in septin localization. Our results do not support a model in which septin nucleotide binding has a specific role in regulating the localization or function of septin-associated proteins.

MATERIALS AND METHODS

Yeast strains, media, and genetic and DNA methods. The *S. cerevisiae* strains used in this study and their construction are described in Table 1. Standard media and molecular biological and genetic methods were used and were described previously (3, 31). Hydroxyurea and α-factor arrest and release were done as described elsewhere (31).

Plasmids. Most plasmids used in this study are listed in Table S1 of the supplemental material; others are described where appropriate below. Oligonucleotide primers used for PCR (see Table S2 in the supplemental material) were purchased from IDT (Coralville, IA), and PCRs were carried out using Expand DNA polymerase (Roche, Indianapolis, IN) as specified by the manufacturer.

Plasmids YEp24/CDC10 and pMS76 were described previously (18, 67). An ~4.2-kb SalI-EcoRI fragment from YEp102(CDC3)2 (47) was subcloned into SalI/EcoRI-digested pALTER (Promega, Madison, WI), yielding pALTER/CDC3. pALTER/CDC3 was digested with SalI followed by partial digestion with XhoI and religation, yielding pALTER/CDC3ΔXhoI, which contains *CDC3* with 940 bp of 5′-flanking DNA. YCp111/CDC3 was generated by cloning an ~3.9-kb EcoRI-PstI fragment from pALTER/CDC3ΔXhoI into EcoRI/PstI-digested YCplac111. YCp111/cdc3G129V, YCp111/cdc3K132T, YCp111/cdc3K132E, YCp111/cdc3T133N, and YCp111/cdc3G129V, K132E, T133N were generated by in vivo recombination of XhoI-digested YCp111/CDC3 with PCR products generated from pRSCDC3 as the template and primer pairs ML388 and ML473, ML434 and ML473, ML389 and ML473, ML390 and ML473, and ML473 and ML474, respectively. YCp111/cdc10G42V and YCp111/cdc10K45T were generated by in vivo recombination of BamHI-digested YCp111/CDC10 with PCR products generated from YEp24/CDC10 as the template and primer pairs ML448/ML615 and ML448/ML651, respectively. YCp111/CDC11 was generated by subcloning an ~4-kb PstI-SalI fragment carrying *CDC11* from plasmid YEPC5#12 (kindly provided by John R. Pringle) into PstI/SalI-digested YCpl ac111. YCp111/cdc11G32V, YCp111/cdc11R35T, YCp111/cdc11R35E, YCp111/cdc11S36N, and YCp111/cdc11G32V, R35E, S36N were generated by in vivo recombination of StuI-digested YCp111/CDC11 with PCR products generated from pRSCDC11 as the template and primer pairs ML393/ML396, ML377/ML396, ML396/ML429, ML396/ML430, and ML396/ML556, respectively. YCp111/cdc11G29D and YCp111/cdc11G32E were generated by in vivo recombination of StuI-digested YCp111/CDC11 with PCR products generated by primers ML396 and ML397 with genomic DNA templates isolated from strains JPT9 (*MAT***a** *cdc11-7*; kindly provided by John R. Pringle) and JPT194-HO1 (1), respectively. YIp211/CDC11, YIp211/cdc11G32V, YIp211/cdc11R35T, YIp211/cdc11R35E, and YIp211/cdc11S36N were generated by cloning PstI-SalI fragments from the cognate YCp111/cdc11 plasmids into PstI/SalI-digested YIplac211 (24). YCp111/cdc11D89A, G92A and YCp111/cdc11K172A, D174A were generated by in vivo recombination of HpaI-digested YCp111/CDC11 with PCR products generated from YIp211/CDC11 as the template and primer pairs ML687/ML691 and ML695/ML696, respectively. YCp111/cdc12G44V, YCp111/cdc12K47T, YCp111/cdc12G44V, K47E, T48N, and YCp111/cdc12D98A, G101A were generated by in vivo recombination of MluI-digested YCp111/CDC12 with PCR products generated from YEp24(CDC12)N as the template and primer pairs ML452/ML616, ML452/ML583, ML452/ML557, and ML949/ML950, respectively.

Plasmids for expression by rabbit reticulocyte lysate coupled in vitro transcription and translation (TnT) were generated as follows. pSP64TT1R1 was generated by in vivo recombination of AatII-digested pSP64T(XSBBSE) with the PCR product generated from YRp7 as the template and primers ML639 and ML640. pSP64TT1R1-6His was generated by in vivo recombination of BamHI-digested pSP64TT1R1 with the PCR product generated by annealing and extension of primers ML641 and ML642. pSP64T1R1-6His/CDC3 was generated by in vivo recombination of XhoI-digested pSP64T1R1-6His with the PCR product generated from YCp111/CDC3 as the template and primers ML677 and ML678. pSP64T1R1-6His/cdc3G129V, K132E, T133N was generated by in vivo recombination of AccB7I-digested pSP64T1R1-6His/CDC3 from the PCR product generated from YCp111/cdc3G129V, K132E, T133N as the template and primers ML392 and ML683. pSP64T(SXBBSE)/CDC10 was generated by PCR from YCp111/CDC10 as the template and primers ML477 and ML478, followed by digestion of the PCR product with XbaI and SacI and ligation into XbaI/SacI-

TABLE 1. *S. cerevisiae* strains used in this study

Strain	Relevant genotype[a]	Source or reference
YEF473	*MAT***a**/α *his3-Δ200/his3-Δ200 leu2-Δ1/leu2-Δ1 lys2-801/lys2-801 trp1-Δ63/trp1-Δ63 ura3-52/ura3-52*	7
YEF473A	*MAT***a** *his3-Δ200 leu2-Δ1 lys2-801 trp1-Δ63 ura3-52*	56
YEF473B	*MAT*α *his3-Δ200 leu2-Δ1 lys2-801 trp1-Δ63 ura3-52*	56
LSY365	*MAT***a** *rsr1*Δ::*HIS3*	J. Pringle
LSY388	*MAT***a**/α *rsr1*Δ::*HIS3*/*rsr1*Δ::*HIS3*	66
HH615	*MAT***a**/α *bud9-Δ1*::*HIS3*/*bud9-Δ1*::*HIS3*	34
M-2772	*MAT*α *cla4*Δ::*HIS3* [YCp111/CDC3-GFP]	Transformant of YEF1343 11
M-3491	*MAT***a** [YCp111/CDC12-YFP]	Transformant of YEF473A
M-3492	*MAT***a** [YCp111/cdc12G44V, K47E, T48N-YFP]	Transformant of YEF473A
M-376	*MAT***a**/α *cdc12*Δ::*TRP1*/*CDC12*	This study[b]
M-377	*MAT***a** *cdc12*Δ::*TRP1* [YEp24(CDC12)N]	This study[c]
YNT107	*MAT***a** *cdc12*Δ::*TRP1* [YCp111/CDC12]	This study[d]
M-2863	*MAT***a** *cdc12*Δ::*TRP1* [YCp111/CDC12] and [pRS316/GFP-CDC3]	Transformant of YNT107
YNT233	*MAT***a** *cdc12*Δ::*TRP1* [YCp111/cdc12G44V]	This study[d]
M-2864	*MAT***a** *cdc12*Δ::*TRP1* [YCp111/cdc12G44V] and [pRS316/GFP-CDC3]	Transformant of YNT233
YNT109	*MAT***a** *cdc12*Δ::*TRP1* [YCp111/cdc12K47T]	This study[d]
M-2865	*MAT***a** *cdc12*Δ::*TRP1* [YCp111/cdc12K47T] and [pRS316/GFP-CDC3]	Transformant of YNT109
YNT131	*MAT***a** *cdc12*Δ::*TRP1* [YCp111/cdc12G44V, K47E, T48N]	This study[d]
M-2866	*MAT***a** *cdc12*Δ::*TRP1* [YCp111/cdc12G44V, K47E, T48N] and [pRS316/GFP-CDC3]	Transformant of YNT131
M-2840	*MAT***a** *cdc12*Δ::*TRP1* [YCp111/cdc12D98A, G101A]	This study[d]
M-2867	*MAT***a** *cdc12*Δ::*TRP1* [YCp111/cdc12D98A, G101A] and [pRS316/GFP-CDC3]	Transformant of M-2840
M-1726	*MAT***a** *cdc12-6*	This study[e]
M-2962	*MAT***a** *cdc12-6* [pRS316/GFP-CDC3]	Transformant of M-1726
M-3489	*MAT***a** [YCp111/CDC10-YFP]	Transformant of YEF473A
M-3490	*MAT***a** [YCp111/cdc10K45T-YFP]	Transformant of YEF473A
DD185	*MAT***a**/α *cdc10*Δ::*HIS3*/*CDC10*	15
M-611	*MAT***a** *cdc10*Δ::*HIS3* [YEp24/CDC10]	This study[f]
YNT89	*MAT***a** *cdc10*Δ::*HIS3* [YCp111]	This study[g]
M-2894	*MAT***a** *cdc10*Δ::*HIS3* [YCp111] and [pRS316/GFP-CDC3]	Transformant of YNT89
YNT91	*MAT***a** *cdc10*Δ::*HIS3* [YCp111/CDC10]	This study[g]
M-2855	*MAT***a** *cdc10*Δ::*HIS3* [YCp111/CDC10] and [pRS316/GFP-CDC3]	Transformant of YNT91
YNT225	*MAT***a** *cdc10*Δ::*HIS3* [YCp111/cdc10G42V]	This study[g]
M-2856	*MAT***a** *cdc10*Δ::*HIS3* [YCp111/cdc10G42V] and [pRS316/GFP-CDC3]	Transformant of YNT225
YNT93	*MAT***a** *cdc10*Δ::*HIS3* [YCp111/cdc10K45T]	This study[g]
M-2857	*MAT***a** *cdc10*Δ::*HIS3* [YCp111/cdc10K45T] and [pRS316/GFP-CDC3]	Transformant of YNT93
M-3487	*MAT***a** [YCp111/CDC3-YFP]	Transformant of YEF473A
M-3488	*MAT***a** [YCp111/cdc3G129V, K132E, T133N-YFP]	Transformant of YEF473A
M-379	*MAT***a**/α *cdc3*Δ::*TRP1*/*CDC3*	This study[b]
M-381	*MAT***a** *cdc3*Δ::*TRP1* [pRSCDC3]	This study[h]
M-438	*MAT***a** *cdc3*Δ::*TRP1* [YCp111/CDC3]	This study[i]
M-2922	*MAT***a** *cdc3*Δ::*TRP1* [YCp111/CDC3] and [pMS76]	Transformant of M-381
M-2914	*MAT***a** *cdc3*Δ::*TRP1* [YCp111/cdc3G129V]	This study[i]
M-2923	*MAT***a** *cdc3*Δ::*TRP1* [YCp111/cdc3G129V] and [pMS76]	Transformant of M-2914
M-2915	*MAT***a** *cdc3*Δ::*TRP1* [YCp111/cdc3K132T]	This study[i]
M-2924	*MAT***a** *cdc3*Δ::*TRP1* [YCp111/cdc3K132T] and [pMS76]	Transformant of M-2915
M-2916	*MAT***a** *cdc3*Δ::*TRP1* [YCp111/cdc3K132E]	This study[i]
M-2925	*MAT***a** *cdc3*Δ::*TRP1* [YCp111/cdc3K132E] and [pMS76]	Transformant of M-2916
M-2917	*MAT***a** *cdc3*Δ::*TRP1* [YCp111/cdc3T133N]	This study[i]
M-2926	*MAT***a** *cdc3*Δ::*TRP1* [YCp111/cdc3T133N] and [pMS76]	Transformant of M-2917
M-2918	*MAT***a** *cdc3*Δ::*TRP1* [YCp111/cdc3G129V, K132E, T133N]	This study[i]
M-2927	*MAT***a** *cdc3*Δ::*TRP1* [YCp111/cdc3G129V, K132E, T133N] and [pMS76]	Transformant of M-2918
M-3474	*MAT***a**/α *cdc3*Δ::*TRP1*/*cdc3*Δ::*TRP1* [YCp111/cdc3G129V, K132E, T133N]	This study[j]
M-3344	*MAT***a**/α [YCp111/CDC11-YFP]	Transformant of YEF473
M-3352	*MAT***a**/α [YCp111/cdc11K172A, D174A-YFP]	Transformant of YEF473
M-2036	*MAT***a**/α *cdc11*Δ::*TRP1*/*CDC11*	This study[b]
M-2283	*MAT***a**/α *cdc11*Δ::*TRP1*/*CDC11 ura3*:*URA3*:*CDC11*/*ura3*	Transformant of M-2036
M-2332	*MAT***a** *cdc11*Δ::*TRP1 ura3*:*URA3*:*CDC11*	Segregant from M-2283
M-2333	*MAT*α *cdc11*Δ::*TRP1 ura3*:*URA3*:*CDC11*	Segregant from M-2283
M-2334	*MAT***a**/α *cdc11*Δ::*TRP1*/*cdc11*Δ::*TRP1 ura3*:*URA3*:*CDC11*/*ura3*:*URA3*:*CDC11*	M-2332 × M-2333
M-2437	*MAT***a** *cdc11*Δ::*TRP1 ura3*:*URA3*:*CDC11* [YCp111/CDC3-GFP]	Transformant of M-2332
M-2297	*MAT***a** $cdc11^{G32E}$	This study[k]
M-2298	*MAT*α $cdc11^{G32E}$	This study[k]
M-2344	*MAT***a**/α $cdc11^{G32E}$/$cdc11^{G32E}$	M-2297 × M-2298
M-2452	*MAT***a** $cdc11^{G32E}$ [YCp111/CDC3-GFP]	Transformant of M-2297
M-3172	*MAT***a** $cdc11^{G32E}$ [pMS76]	Transformant of M-2297
M-3174	*MAT***a** $cdc11^{G32E}$ *cdc3*Δ::*TRP1* [YCp111/cdc3K132T] and [pMS76]	This study[j]
M-2042	*MAT***a**/α *cdc11*Δ::*TRP1*/*CDC11 ura3*:*URA3*:$cdc11^{G32V}$/*ura3*	Transformant of M-2036
M-2323	*MAT***a** *cdc11*Δ::*TRP ura3*:*URA3*:$cdc11^{G32V}$	Segregant from M-2042
M-2324	*MAT*α *cdc11*Δ::*TRP ura3*:*URA3*:$cdc11^{G32V}$	Segregant from M-2042
M-2325	*MAT***a**/α *cdc11*Δ::*TRP1*/*cdc11*Δ::*TRP1 ura3*:*URA3*:$cdc11^{G32V}$/*ura3*:*URA3*:$cdc11^{G32V}$	M-2323 × M-2324
M-2440	*MAT***a** *cdc11*Δ::*TRP ura3*:*URA3*:$cdc11^{G32V}$ [YCp111/CDC3-GFP]	Transformant of M-2323
M-2723	*MAT***a** *cdc11*Δ::*TRP ura3*:*URA3*:$cdc11^{G32V}$ *cla4*Δ::*HIS3* [YCp111/CDC3-GFP]	This study[n]
M-2275	*MAT***a**/α *cdc11*Δ::*TRP1*/*CDC11 ura3*:*URA3*:$cdc11^{R35T}$/*ura3*	Transformant of M-2036
M-2311	*MAT***a** *cdc11*Δ::*TRP1 ura3*:*URA3*:$cdc11^{R35T}$	Segregant from M-2275
M-2312	*MAT*α *cdc11*Δ::*TRP1 ura3*:*URA3*:$cdc11^{R35T}$	Segregant from M-2275
M-2313	*MAT***a**/α *cdc11*Δ::*TRP1*/*cdc11*Δ::*TRP1 ura3*:*URA3*:$cdc11^{R35T}$/*ura3*:*URA3*:$cdc11^{R35T}$	M-2311 × M-2312
M-2443	*MAT***a** *cdc11*Δ::*TRP1 ura3*:*URA3*:$cdc11^{R35T}$ [YCp111/CDC3-GFP]	Transformant of M-2311
M-2726	*MAT***a** *cdc11*Δ::*TRP ura3*:*URA3*:$cdc11^{R35T}$ *cla4*Δ::*HIS3* [YCp111/CDC3-GFP]	This study[n]
M-2273	*MAT***a**/α *cdc11*Δ::*TRP1*/*CDC11 ura3*:*URA3*:$cdc11^{R35E}$/*ura3*	Transformant of M-2036
M-2299	*MAT***a** *cdc11*Δ::*TRP1 ura3*:*URA3*:$cdc11^{R35E}$	Segregant from M-2273

Continued on following page

TABLE 1—*Continued*

Strain	Relevant genotype[a]	Source or reference
M-2300	*MAT*α *cdc11*Δ::*TRP1 ura3*:*URA3*:*cdc11*^{R35E}	Segregant from M-2273
M-2301	*MAT***a**/α *cdc11*Δ::*TRP1*/*cdc11*Δ::*TRP1 ura3*:*URA3*:*cdc11*^{R35E}/*ura3*:*URA3*:*cdc11*^{R35E}	M-2299 × M-2300
M-2446	*MAT***a** *cdc11*Δ::*TRP1 ura3*:*URA3*:*cdc11*^{R35E} [YCp111/CDC3-GFP]	Transformant of M-2299
M-2776	*MAT***a** *cdc11*Δ::*TRP1 ura3*:*URA3*:*cdc11*^{R35E} *cla4*Δ::*HIS3* [YCp111/CDC3-GFP]	This study[o]
M-2274	*MAT***a**/α *cdc11*Δ::*TRP1*/*CDC11 ura3*:*URA3*:*cdc11*^{S36N}/*ura3*	Transformant of M-2036
M-2305	*MAT***a** *cdc11*Δ::*TRP1*/*CDC11 ura3*:*URA3*:*cdc11*^{S36N}	Segregant from M-2274
M-2306	*MAT*α *cdc11*Δ::*TRP1*/*CDC11 ura3*:*URA3*:*cdc11*^{S36N}	Segregant from M-2274
M-2307	*MAT***a**/α *cdc11*Δ::*TRP1*/*cdc11*Δ::*TRP1 ura3*:*URA3*:*cdc11*^{S36N}/*ura3*:*URA3*:*cdc11*^{S36N}	M-2305 × M-2306
M-2449	*MAT***a** *cdc11*Δ::*TRP1*/*CDC11 ura3*:*URA3*:*cdc11*^{S36N} [YCp111/CDC3-GFP]	Transformant of M-2305
M-367	*MAT***a** *cdc11*Δ::*TRP1* [pRSCDC11]	This study[p]
M-368	*MAT*α *cdc11*Δ::*TRP1* [pRSCDC11]	This study[p]
M-432	*MAT***a**/α *cdc11*Δ::*TRP*/*cdc11*Δ::*TRP1* [pRSCDC11]	M-367 × M-368
YNT95	*MAT***a** *cdc11*Δ::*TRP1* [YCplac111]	This study[q]
M-2897	*MAT***a** *cdc11*Δ::*TRP1* [YCplac111] and [pRS316/GFP-CDC3]	Transformant of YNT95
YNT97	*MAT***a** *cdc11*Δ::*TRP1* [YCp111/CDC11]	This study[q]
M-3367	*MAT***a** *cdc11*Δ::*TRP1* [YCp111/CDC11-YFP]	This study[q]
M-2365	*MAT***a** *cdc11*Δ::*TRP1* [YCp111/cdc11G29D]	This study[q]
M-2859	*MAT***a** *cdc11*Δ::*TRP1* [YCp111/cdc11G29D] and [pRS316/GFP-CDC3]	Transformant of M-2365
YNT195	*MAT***a** *cdc11*Δ::*TRP1* [YCp111/cdc11G32V, R35E, S36N]	This study[q]
M-2860	*MAT***a** *cdc11*Δ::*TRP1* [YCp111/cdc11G32V, R35E, S36N] and [pRS316/GFP-CDC3]	Transformant of YNT195
M-3214	*MAT***a** *cdc11*Δ::*TRP1* [YCp111/cdc11D89A, G92A]	This study[q]
M-3277	*MAT***a** *cdc11*Δ::*TRP1 CDC3*:*URA3*:*CDC3-GFP* [YCp111/cdc11D89A, G92A]	Transformant of M-3214[r]
M-3186	*MAT***a**/α *cdc11*Δ::*TRP*/*cdc11*Δ::*TRP1* [YCp111/cdc11D89A, G92A]	This study[s]
M-3258	*MAT***a** *cdc11*Δ::*TRP1* [YCp111/cdc11K172A, D174A]	This study[q]
M-3374	*MAT***a** *cdc11*Δ::*TRP1* [YCp111/cdc11K172, D174A-YFP]	This study[q]
M-3280	*MAT***a** *cdc11*Δ::*TRP1 CDC3*:*URA3*:*CDC3-GFP* [YCp111/cdc11K172A, D174A]	Transformant of M-3258[r]
M-3472	*MAT***a** *cdc11*Δ::*TRP1 CDC3*:*URA3*:*CDC3-GFP cla4*Δ::*HIS3* [YCp111/cdc11K172A, D174A]	This study[s]
M-3473	*MAT***a**/α *cdc11*Δ::*TRP*/*cdc11*Δ::*TRP1* [YCp111/cdc11G32V, R35E, S36N]	This study[t]
M-2618	*MAT*α *cdc11*$^{G32E\text{-}3HA}$	Transformant of M-2298[u]
M-2630	*MAT***a**/α *cdc11*$^{G32E\text{-}3HA}$/*cdc11*^{G32E}	M-2618 × M-2297
M-2634	*MAT***a**/α *cdc11*$^{G32E\text{-}3HA}$/*CDC11*	M-2618 × YEF473A
M-2159	*MAT*α *CDC11-*^{3HA}	Transformant of YEF473B[u]
M-2633	*MAT***a**/α *CDC11-*^{3HA}/*CDC11*	M-2159 × YEF473A
EGY48R	*MAT***a** *his3 trp1 ura3-52* [pSH18-34]	78[v]

[a] Except for strain EGY48R, all strains are congenic with YEF473. Plasmids are indicated by square brackets.
[b] *CDC3*, *CDC11*, and *CDC12* were deleted in strain YEF473, as described previously (22).
[c] Segregant from M-376 transformed with YEp24(CDC12)N.
[d] Strain M-377 was transformed with the indicated *LEU2* plasmid and plated on medium lacking leucine and containing 0.1% 5-fluoroorotic acid to select for loss of YEp24(CDC12)N.
[e] Derived from backcrossing the *cdc12-6* strain M-238 (56) 10 times into the YEF473 strain background.
[f] Segregant from DD185 transformed with YEp24/CDC10.
[g] Strain M-611 was transformed with the indicated *LEU2* plasmid and plated on medium lacking leucine and containing 0.1% 5-fluoroorotic acid to select for loss of YEp24/CDC10.
[h] Segregant from M-379 transformed with pRSCDC3.
[i] Strain M-381 was transformed with the indicated *LEU2* plasmid and plated on medium lacking leucine and containing 0.1% 5-fluoroorotic acid to select for loss of pRSCDC3.
[j] Derived from mating segregants from M-379 transformed with pRSCDC3, followed by transformation with YCp111/cdc3G129V, K132E, T133N and plating on medium lacking leucine and containing 0.1% 5-fluoroorotic acid to select for loss of pRSCDC3.
[k] Derived from backcrossing the *cdc11-6* strain JPT194 (1) 10 times into the YEF473 strain background.
[l] Segregant from cross of M-2298 and M-2925.
[m] Segregant from cross of M-2440 and M-2772.
[n] Segregant from cross of M-2443 and M-2772.
[o] Segregant from cross of M-2446 and M-2772.
[p] Segregant from M-2036 transformed with pRSCDC11.
[q] Strain M-367 was transformed with the indicated *LEU2* plasmid and plated on medium lacking leucine and containing 0.1% 5-fluoroorotic acid to select for loss of pRSCDC11.
[r] Transformed with ApaI-digested YIp211/CDC3-GFP.
[s] Segregant from cross of M-3280 and YEF1373.
[t] Strain M-432 was transformed with YCp111/cdc11K172A, D174A and plated on medium lacking leucine and containing 0.1% 5-fluoroorotic acid to select for loss of pRSCDC11.
[u] Transformed with the PCR product of primers ML298 and ML299 using as template pFA6a-3HA-His3MX6 (57).
[v] pSH18-34 is a 2μm *URA3* plasmid with an *8lexOp-lacZ* reporter gene (3).

digested pSP64T(SXBBSE). pSP64T1R1/CDC10 was generated by in vivo recombination of AatII-digested pSP64T(SXBBSE)/CDC10 with the PCR product generated from YRp7 as the template and primers ML639 and ML640. psP64TT 1R1/CDC10G42V was generated by in vivo recombination of BamHI/BglII-digested YCp111/cdc10G42V and BspE1-digested psP64TT1R1/CDC10. pSP 64T(SXBBSE)/cdc11G29D, pSP64T(SXBBSE)/cdc11G32E, pSP64T(SXBBSE)/ cdc11G32V, pSP64T(SXBBSE)/cdc11R35T, pSP64T(SXBBSE)/cdc11R35E, pSP64T(SXBBSE)/cdc11S36N, and pSP64T(SXBBSE)/cdc11G32V, R35E, S36N were generated by PCR from the cognate YCp111/cdc11 plasmids as the template and primers ML566 and ML621, digestion of the resulting PCR products with BglII and MfeI, and ligation into BglII/MfeI-digested pSP64T(SXB BSE)/CDC11. pSP64T1R1/CDC11 was generated by in vivo recombination of AatII-digested pSP64T(SXBBSE)/CDC11 with the PCR product from YRp7 as the template and primers ML639 and ML640. pSP64T1R1-6His/CDC11 and pSP64T1R1-6His/CDC11-C were generated by in vivo recombination of XhoI-digested pSP64T1R1-6His with PCR products generated from YCp111/CDC11 as the template and primer pairs ML668/ML671 and ML670/ML671, respectively. pSP64T1R1-6His/CDC11-N, pSP64T1R1-6His/cdc11G32E-N, pSP64 T1R1-6His/cdc11G32V-N, pSP64T1R1-6His/cdc11R35T-N, and pSP64T1R1-6His/cdc11R35E-N were generated by in vivo recombination of XhoI-digested pSP64T1R1-6His with the PCR products generated from the cognate YCp111/cdc11 plasmids as the template and primers ML668 and ML669. pSP64T1R1/CDC12 was generated by in vivo recombination of AatII-digested pSP64T(SXB BSE)/CDC12 with the PCR product generated from YRp7 as the template and primers ML639 and ML640. pSP64T1R1-6His/CDC12, pSP64T1R1-6His/CDC12-N, and pSP64T1R1-6His/CDC12-C were generated by in vivo recombi-

nation of XhoI-digested pSP64T1R1-6His with the PCR products generated from YCp111/CDC12 as the template and primer pairs ML672/ML675, ML672/ML673, and ML674/ML675, respectively. pSP64T1R1/cdc12G44V and pSP64 T1R1/cdc12G44V, K47E, T48N were generated by in vivo recombination of BstBI-digested pSP64T1R1/CDC12 with EcoRV/XbaI-digested YCp111/cdc12G44V and YCp111/cdc12G44V, K47E, T48N, respectively. pSP64T1R1/cdc12S43V was generated by in vivo recombination of MluI-digested pSP64 T1R1/CDC12 with the PCR product generated from YCp111/CDC12 as the template and primers ML452 and ML947.

Plasmids for two-hybrid assays were generated as follows. pEG202/cdc3G129V, pEG202/cdc3K132T, pEG202/cdc3T133N, and pEG202/cdc3G129V, K132E, T133N were generated by in vivo recombination of PvuII-digested pEG202/CDC3 with the PCR products generated from the cognate YCp111/cdc3 plasmids as the template and primers ML392 and ML683. pEG202/cdc10K45T was generated by in vivo recombination of BspE1-digested pEG202/CDC10 with BamHI/BglII-digested YCp111/cdc10K45T. pEG202/cdc11G32V, pEG202/cdc11R35T, pEG202/cdc11R35E, pEG202/cdc11S36N, and pEG202/cdc11G32V, R35E, S36N were generated by in vivo recombination of NotI/BspEI-digested pEG202/CDC11 with the PCR products generated from the cognate YCp111/cdc11 plasmids as the template and primers ML397 and ML582. pEG202/cdc11D89A, G92A and pEG202/cdc11K172A, D174A were generated by in vivo recombination of NotI/BspEI-digested pEG202/CDC11 with the PCR products generated from the cognate YCp111/cdc11 plasmids as the template and primers ML582 and ML747. pEG202/cdc12S43V was generated by in vivo recombination of PflMI-digested pEG202/CDC12 with pSP64T1R1/cdc12S43V digested with BamHI/HpaI. pEG202/cdc12G44V and pEG202/cdc12G44V, K47E, T48N were generated by in vivo recombination of PflMI-digested pEG202/CDC12 with the cognate YCp111/cdc12 plasmids digested with EcoRV and XbaI. pJG4-5/cdc11 G32V, pJG4-5/cdcR35T, pJG4-5/cdc11R35E, pJG4-5/cdc11S36N, and pJG4-5/cdc11G32V, R35E, S36N were generated by in vivo recombination of BspEI-digested pJG4-5/CDC11 with the PCR products generated from the cognate YCp111/cdc11 plasmids as the template and primers ML397 and ML622.

Plasmids for expressing yellow fluorescent protein (YFP)-tagged wild-type and P-loop mutant septins in in vivo competition assays were generated as follows. YCp111/CDC3-YFP and YCp111/cdc3G129V, K132E, T133N-YFP were generated by in vivo recombination of the PCR products generated by primers ML1003 and ML1066 with pKT139 (68) as the template with YCp111/CDC3 and YCp111/cdc3G129V, K132E, T133N, respectively. YCp111/CDC10-YFP and YCp111/cdc10K45T-were generated by in vivo recombination of the PCR products from pDH5 as the template (http://depts.washington.edu/~yeastrc/pages/fm_home2.html) and primers ML295 and ML296 and cotransformation with YCp111/CDC10 and YCp111/cdc10K45T, respectively. YCp111/CDC11-YFP and YCp111/cdc11K172A, D174A-YFP were generated by in vivo recombination of the PCR product generated from pKT139 as the template and primers ML1058 and ML1059 with PacI-digested YCp111/CDC11 and YCp111/cdc11 K172A, D174A, respectively. YCp111/CDC12-YFP and YCp111/cdc12G44V, K47E, T48N-YFP were generated by in vivo recombination of the PCR product generated from pKT139 as the template and primers ML1063 and ML1064 with pKT139 and cotransformation with YCp111/CDC12 and YCp111/cdc12G44V, K47E, T48N, respectively.

Microscopy. Fluorescence and differential interference contrast still microscopy were done using a Nikon Eclipse E800 microscope and a Hamamatsu Orca ERII charge-coupled-device camera. Images were acquired using Metamorph software (Molecular Devices, Sunnyvale, CA) and processed using Image J (Wayne Rasband; NIH; http://rsb.info.nih.gov/ij/). For the quantitation of YFP-tagged septin localization to the neck (see Fig. 5B, below), identical exposures were taken in the YFP channel of wild-type and mutant medium-budded cells. The maximum intensity pixel in a 2-μm by 2-μm rectangle over the neck region was determined for >200 cells/sample. When observed with the camera, YFP-tagged septins were detectable at >95% of the necks of M-3367, M-3344, M-3374, M-3487, M-3489, M-3490, and M-3491 cells at 23°C and of M-3489 cells at 27°C. YFP-tagged septins were detectable in ~80% of M-3488 cells and in ~25% of M-3492 cells at 23°C. For these strains, only cells that contained fluorescence above background were used for quantitation. At 23°C, <1% of M-3352 cells had neck-localized septins detectable by the camera. In this strain, the intensity at the neck was determined whether or not the signal was above background. Background was determined using YEF473, and the average background intensity was subtracted from the intensity of the YFP-tagged strains. To evaluate bud site selection, chitin was detected using Calcofluor white (31) and cells with three or more bud scars were scored, with cells scored as budding axially if all bud scars were in a single chain emanating from one cell pole and as budding bipolarly if all bud scars were at either of the cell poles.

Movies were acquired using a spinning disc confocal microscope as described elsewhere (10), except *Z*-series of 10 focal planes 0.5 μm apart were collected at 2-min intervals, collapsed into a single two-dimensional image using a maximum-value projection, and processed using Image J.

Immunofluorescence and immunoblotting. Primary antibodies used included a monoclonal mouse antihemagglutinin (anti-HA) antibody (Covance, Princeton, NJ) and polyclonal rabbit anti-Cdc11p and goat anti-Cdc10p antibodies (Santa Cruz Biotechnology, Santa Cruz, CA). Polyclonal rabbit anti-Cdc3p and anti-Cdc12p antibodies were raised against Cdc3p (CNHSPVPTKKKGFLR) and Cdc12p (CEQVKSLQVKKSHLK) C-terminal peptides and affinity purified against the antigenic peptide (Sigma/Genosys, Woodlands, TX). Secondary antibodies for immunoblotting included horseradish peroxidase-conjugated donkey anti-rabbit immunoglobulin G (IgG), sheep anti-mouse antibody (Amersham Biosciences, Arlington Heights, IL), and rabbit anti-goat antibody (Jackson ImmunoResearch Laboratories, West Grove, PA). Immunofluorescence was done as described previously (65) using anti-Cdc11p or anti-HA primary antibodies and Alexa 540-conjugated goat anti-rabbit IgG or Alexa 488-conjugated goat anti-mouse IgG secondary antibodies (Molecular Probes, Eugene, OR).

Protein preparation and analysis of protein-protein interactions. Cells were grown to mid-log phase in yeast extract-peptone-dextrose or the appropriate selective medium, and cells (optical density at 600 nm of 25) were harvested. Cell pellets were resuspended in 500 μl BB buffer (25 mM HEPES pH 7.4, 150 mM NaCl, 0.1% Triton X-100, 5 mM $MgCl_2$, 10% glycerol) supplemented with a protease inhibitor cocktail and phenylmethylsulfonyl fluoride (Sigma, St. Louis, MO), lysed at 4°C with 250 μl of ~0.5-mm glass beads by vortexing, and centrifuged at 13,000 × *g* for 10 min to remove cell debris, and protein amounts were quantitated using the Bio-Rad protein assay (Bio-Rad Laboratories, Hercules, CA). For immunoblotting of total protein samples, Laemmli sample buffer was added to 80 μg protein, samples were heated for 5 min and centrifuged for 5 min prior to separation on 10% sodium dodecyl sulfate-polyacrylamide gel electrophoresis (SDS-PAGE) gels and transfer to polyvinylidene difluoride (PVDF) membrane. Equal loading was verified by Ponceau S staining of the PVDF membrane. Specific proteins were detected using the appropriate primary and secondary antibodies and an enhanced chemiluminescence system (Amersham).

For immunoprecipitations, 30 μl of protein G beads and 2 μg primary antibody were added to extract containing 1.5 mg of protein followed by incubation at 4°C for 2.5 h. The beads were pelleted at 4°C and washed four times with BB, and one-half of the sample was analyzed by immunoblotting. Two-hybrid analyses were done as described previously (53). For analysis of septin-septin interactions in vitro, ^{35}S-labeled proteins were synthesized in 25-μl rabbit reticulocyte lysate-coupled in vitro TnT reaction mixtures, as described elsewhere (41). Immunoblotting and comparison to quantitated *E. coli*-produced septins indicated that ~80 ng of each septin was synthesized per reaction mixture. Septins were allowed to interact for 1 h at 23°C followed by the addition of 1 μg of anti-Cdc11p or anti-Cdc12p antibodies and 20 μl protein G beads and incubated for 1 h. Beads were pelleted, and 5 μl of the supernatant was saved as the unbound fraction. The beads were washed four times with IP150 [20 mM piperazine-*N*,*N*′-bis(2-ethanesulfonic acid) pH 7.5, 150 mM NaCl, 0.5% Tween 20], yielding the bound fraction. Analysis of interactions using six-His-tagged septins was as described above except that proteins were bound to 20 μl Talon beads (BD Biosciences, Palo Alto, CA) and 10 mM imidazole was present during the incubation and washes. Following SDS-PAGE, proteins were transferred to a PVDF membrane and detected by autoradiography.

Modeling of yeast septin structures. Alignments and secondary structure predictions shown in Fig. S3 at http://www.cooperlab.wustl.edu/restricted/marklongtine/ were generated using Clustal W (13; http://npsa-pbil.ibcp.fr/cgi-bin/npsa_automat.pl?page=/NPSA/npsa_clustalw.html) using default parameters. Three crystal structures of septins are available in the RSCB Protein Data Bank (PDB). The structure of a Sept2 dimer bound to GDP (2QA5; 3.4-Å resolution) and of a nucleotide-bound complex of Sept2, Sept6, and Sept7 (2QAG; 4-Å resolution) were deposited by Sirajuddin et al. (70), and an unpublished structure of Sept2 bound to GDP (2QNR; 2.4-Å resolution) was deposited by Rabeh and colleagues. Because of its high resolution and superior structural coverage, the 2QNR Sept2 polypeptide sequence and crystal structure were used for modeling the structures of Cdc11p and Cdc12, as shown in Fig. S4 at http://www.cooperlab.wustl.edu/restricted/marklongtine/ using MODELLER (61) (http://salilab.org/modeler/), and images were generated using VMD (38) (http://www.ks.uiuc.edu/Research/vmd/).

UV cross-linking. Septin complexes were purified from yeast as described previously (22). Briefly, 20 mg yeast protein extract was incubated with 8 μg anti-Cdc3p antibodies followed by elution for 18 h at 4°C in elution buffer (20 mM Tris-HCl, pH 7.8, 1 M KCl, 2 mM $MgCl_2$, 0.5 mM EGTA, 4% sucrose) with 0.8 mg/ml Cdc3p peptide and dialysis against elution buffer. Septins were cross-linked to nucleotide by UV light in the presence of 2 μM [α-^{32}P]GTP and 300

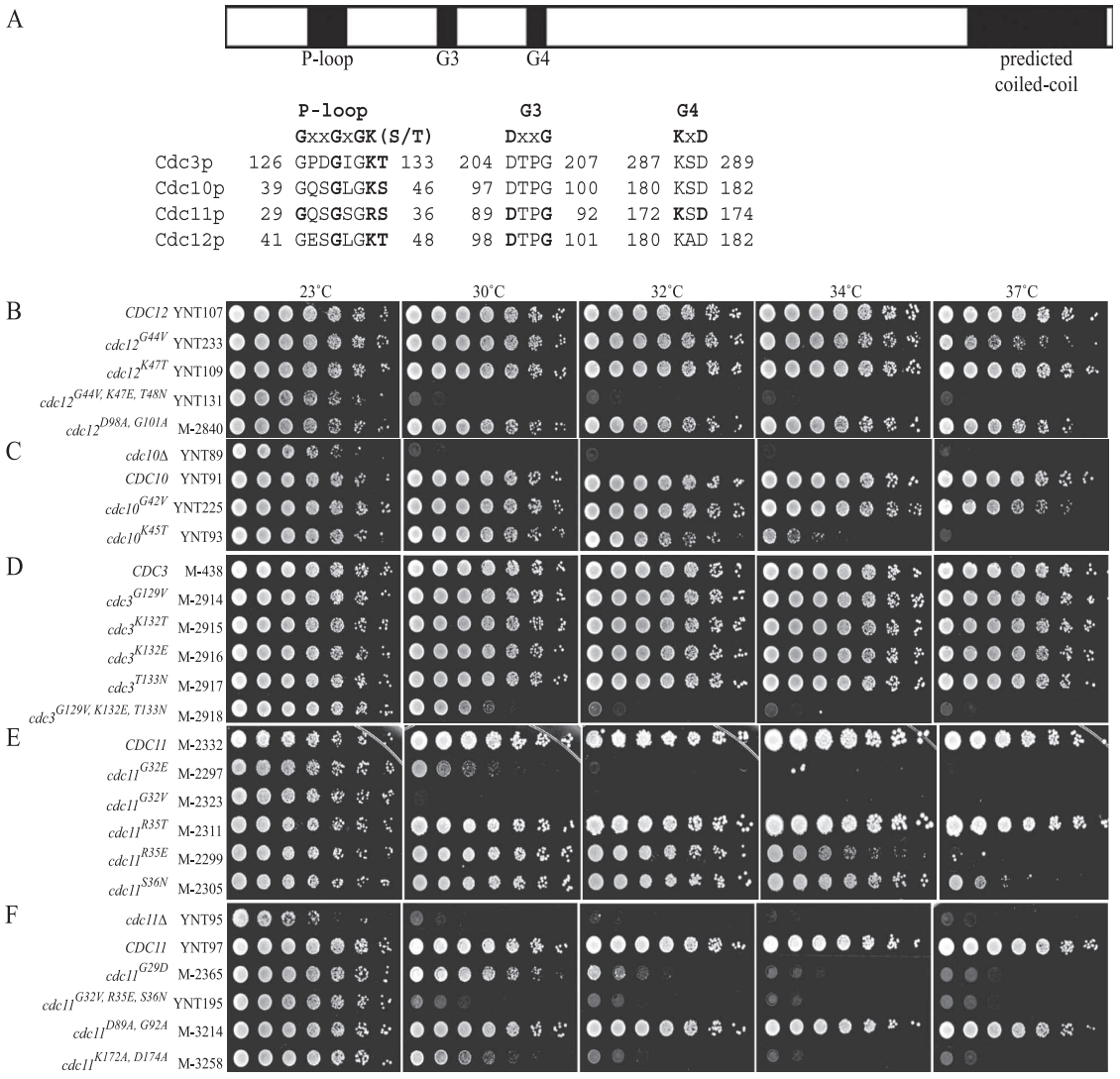

FIG. 1. Effects of mutations in septin nucleotide-binding motifs on cell viability. (A) Schematic diagram of a typical septin. Filled boxes show the approximate locations of septin P-loop, G3, and G4 domains and of the C-terminal predicted coiled-coil region. Indicated are the amino acid sequences of the septin P-loop, G3, and G4 motifs. A bold font indicates residues mutated singly or in combination in this study. (B to F) Viability of wild-type and mutant strains. Strains were grown to mid-log phase in SDC-Leu medium (B to D and F) or YM-P medium (E), and fivefold serial dilutions were plated on the appropriate plates followed by incubation at the indicated temperature for 4 days.

μM nonradioactive ATP at 23°C as described elsewhere (76). A 10% portion of the cross-linked sample was subjected to SDS-PAGE and silver staining, with the remainder subjected to SDS-PAGE, transfer to a PVDF membrane, and autoradiography. The addition of 5 mM EDTA or an additional 300 μM of nonradioactive GTP, but not of nonradioactive ATP, prevented UV cross-linking.

RESULTS

Mutations in septin P-loop and G4 motifs result in temperature-sensitive cell viability, morphogenesis, and division. The central septin G domain contains three motifs (Fig. 1A) conserved in many GTP-binding proteins (reviewed in references 12 and 73). The P-loop [consensus sequence GXXGXGK(S/T)] envelops the phosphates of the bound nucleotide with the glycines necessary to allow the required sharp turn. Typically, the lysine interacts with the nucleotide phosphates and the serine/threonine is involved in Mg^{2+} coordination. In the G3 motif (consensus sequence DXXG), the aspartate typically is involved in Mg^{2+} coordination and the glycine bonds with the γ-phosphate. Residues of the G4 motif (consensus sequence KXD) interact with the nucleotide base and provide specificity for binding to guanine nucleotides. Typically, mutations in the P-loop and G3 motifs reduce GTP binding, although G3 mutations can also affect GTP hydrolysis. Mutations in the G4 motif can allow binding to nonnative nucleotides in vitro and dramatically reduce the ability to bind guanine nucleotides in vivo.

The recently solved 3.4-Å-resolution crystal structure of GDP-bound human Sept2 reveals that the septin G domain structure contains a core of six β-strands and five α-helices and forms a tertiary structure highly similar to that of canonical small GTPases, such as Ras (70) (see Fig. S4 at http://www.cooperlab.wustl.edu/restricted/marklongtine/ with several sep-

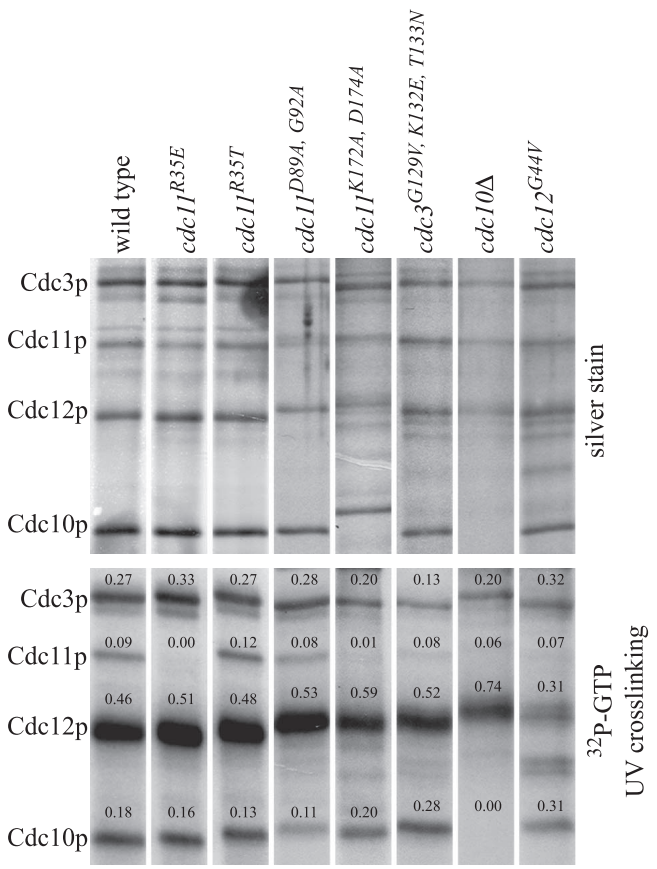

FIG. 2. UV cross-linking of [α-^{32}P]GTP to wild-type and mutant septins purified from yeast. Strains were grown to mid-log phase at 23°C as described for Fig. 1, and septin complexes were purified using anti-Cdc3p antibodies. Septins were incubated with 2 μM [α-^{32}P]GTP and 300 μM ATP, followed by cross-linking with UV light. (Upper panel) Silver-stained SDS-PAGE gel of 10% of the purified sample. (Lower panel) Autoradiography of the remaining sample to detect cross-linked GTP. Numbers represent the fractions of total [^{32}P]GTP in the indicated band.

tin-unique structural elements flanking the septin G domain (70) (see Fig. S3 at http://www.cooperlab.wustl.edu/restricted/marklongtine/. Both the Sept2-GDP structure solved by Sirajuddin (PDB accession 2QA5) and an unpublished, 2.4-Å-resolution Sept2-GDP crystal structure by Rabeh and colleagues (PDB accession 2QNR) show that in mammalian septins, as in canonical small GTPases, the P-loop envelops the nucleotide, the G3 motif is positioned near the γ-phosphate, and the G4 motif is juxtaposed to the guanine base. We found that Cdc11p, Cdc12p, Cdc3p, and Cdc10p are predicted to contain the same secondary structures as mammalian Sept2 (data not shown; see Fig. S3 at http://www.cooperlab.wustl.edu/restricted/marklongtine/). Modeling of the structures of Cdc11p and Cdc12p on the high-resolution Sept2-GDP structure using MODELLER (61) suggests yeast septins, like mammalian septins, bind nucleotides in a conventional manner (see Fig. S4 at http://www.cooperlab.wustl.edu/restricted/marklongtine/).

Previous work has yielded conflicting results on whether or not Cdc3p, Cdc10p, Cdc11p, and Cdc12 all bind GTP (see the introduction). Thus, we first asked if these septins bind GTP (Fig. 2). We isolated septin complexes from yeast and assessed the purification by silver staining and the migration of Cdc3p, Cdc10p, Cdc11p, and Cdc12p by immunoblotting (data not shown). Complexes were incubated with [α-^{32}P]GTP, exposed to UV light, and separated by SDS-PAGE, and GTP-cross-linked proteins were detected by autoradiography. We found that all four septins bound GTP, in agreement with the findings of two other groups (19, 76). Cdc12p accounted for ~46% of the cross-linked GTP, and Cdc3p, Cdc11p, and Cdc10p accounted for ~27%, ~9%, and ~18%, respectively. Because the rate and efficiency of nucleotide exchange and binding and covalent bond formation are unlikely to be identical for each septin, the different levels of cross-linking cannot be interpreted as resulting from differences in binding affinities for GTP. Cross-linking was inhibited by EDTA and competed by GTP but not ATP (data not shown) (see Materials and Methods), as found previously (76).

To investigate the role of nucleotide binding in septin function, we took a mutational approach (Fig. 1A). For each septin, we generated P-loop single-point-mutant alleles, which were expected to reduce GTP binding to variable extents, and a P-loop triple-point-mutant allele, which was expected to eliminate GTP binding (9). We also generated G3 motif mutations in Cdc11p and Cdc12p and a G4 motif mutation in Cdc11p. A subset of these mutations was assayed in the UV cross-linking assay (Fig. 2). A Cdc12 P-loop point mutation (cdc12p^{G44V}) disrupted GTP binding, consistent with reduced GTP binding by *E. coli*-expressed cdc12p^{T48N} (75). P-loop mutations in Cdc11p and Cdc3p also reduced GTP binding (cdc11p^{R35E} and cdc3p$^{G129V,\ K132E,\ T133N}$), while the cdc11p^{R35T} P-loop mutation did not detectably reduce GTP binding in this assay. The residual binding by the band containing cdc3p$^{G129V,\ K132E,\ T133N}$ may be due, at least in part, to comigrating Shs1p (76). Mutation of the G4 motif also reduced GTP binding (cdc11p$^{K172A,\ D197A}$), but surprisingly, mutation of the G3 motif did not (cdc11p$^{D89A,\ G92A}$).

We next investigated the effects of mutations in the septin P-loop, G3, and G4 motifs on cell viability, division, and morphogenesis. *cdc10*Δ strains have reduced viability at 23°C and are inviable at 30°C and above (Fig. 1C; see also Fig. S1B in the supplemental material) (15, 22), and *cdc12*Δ strains are inviable under all conditions (22). A *cdc12*$^{D98A,\ G101}$ G3 motif mutant displayed wild-type viability, division, and morphogenesis at all temperatures (Fig. 1B; see also Fig. S1A in the supplemental material). In a previous study, *cdc10*^{S46N} and *cdc12*^{T48N} mutants displayed temperature-sensitive (Ts) phenotypes, with a *cdc10*^{S46N} *cdc12*^{T48N} double-mutant strain having reduced viability and strong defects in cell division and morphogenesis at 37°C (75). We found similar Ts phenotypes in *cdc10* and *cdc12* P-loop point mutation strains (Fig. 1B; see also Fig. S1A and B, *cdc10*^{G42V}, *cdc10*^{K45T}, and *cdc12*^{G44V}, in the supplemental material). A *cdc12*$^{G44V,\ K47E,\ T48N}$ triple P-loop point mutation strain had a lower minimal restrictive temperature for viability than *cdc12* single P-loop point mutation strains but showed normal viability, division, and morphogenesis at 23°C (Fig. 1B; see also Fig. S1A, *cdc12*$^{G44V,\ K47E,\ T48N}$, in the supplemental material). If this mutation eliminates GTP binding, as expected, this result suggests the Ts phenotypes result from a temperature-sensitive requirement for

nucleotide binding rather than a temperature-sensitive defect in nucleotide binding.

Cdc3p is essential under all conditions, and in our strain background *cdc11*Δ cells have reduced viability at 23°C and are inviable at 30°C and above (Fig. 1F) (22). At 23°C, all *cdc3* and *cdc11* mutants, including the P-loop triple mutants, displayed normal viability, division, and morphogenesis (Fig. 1D to F; see also Fig. S1B to D in the supplemental material). At 37°C, a *cdc11* G3 motif mutant ($cdc11^{D89A,\ G92A}$), a $cdc11^{R35T}$ mutant, and all three *cdc3* P-loop single-point-mutants appeared normal (Fig. 1C and E; see also Fig. S1C and D in the supplemental material). However, the *cdc3* triple P-loop mutant ($cdc3^{G129V,\ K132E,\ T133N}$) (Fig. 1C and D; see also Fig. S1C and D in the supplemental material), the *cdc11* G4 motif mutant, and remaining *cdc11* P-loop mutants displayed Ts viability, division, and morphogenesis ($cdc11^{K172A,\ D174A}$, $cdc11^{G32V}$, $cdc11^{R35E}$, $cdc11^{S36N}$, and $cdc11^{G32V,\ R35E,\ S36N}$) (Fig. 1E and F; see also Fig. S1C in the supplemental material). The minimal restrictive temperatures for viability of these strains ($cdc11^{G32V,\ R35E,\ S36N} = cdc11^{G32V} < cdc11^{K172A,\ D174A} < cdc11^{R35E} \approx cdc11^{S36N} < cdc11^{R35T} = cdc11^{D89A,\ G92A}$) fits well with the expected defects in GTP binding, with $cdc11^{G32V,\ R35E,\ S36N}$ expected to have the greatest reduction in GTP binding and with $cdc11p^{R35E}$, which has undergone a change in residue charge, expected to have greater reduction in nucleotide binding than $cdc11p^{R35T}$. We then asked if the previously identified Ts *cdc11-1*, *cdc11-6*, and *cdc11-7* alleles (1, 36) contain mutations in conserved GTP-binding motifs. DNA sequencing of the entire coding region identified a single mutation in each allele, which is in the P-loop: *cdc11-1* and *cdc11-7* (GGC → G<u>A</u>C) encode $Cdc11p^{G29D}$, and *cdc11-6* (GGA → G<u>A</u>A) encodes $Cdc11p^{G32E}$. When introduced into *CDC11* and expressed in a *cdc11*Δ background (see Materials and Methods), these mutations conferred temperature-sensitive viability, division, and morphogenesis (Fig. 1F and data not shown).

All Cdc3p, Cdc10p, Cdc11p, and Cdc12p mutant proteins were expressed at normal levels at 23°C and 37°C (see Fig. S1E in the supplemental material), indicating the phenotypes are not due to protein instability. All phenotypes were recessive, and we observed no differences in viability, division, or morphogenesis among mutant haploid strains of either mating type or of mutant diploid strains. In summary, our results suggest that Cdc3p, Cdc10p, Cdc11p, and Cdc12p all bind GTP, that the P-loop and G4 motifs are important for nucleotide binding, and that nucleotide binding is important for septin function in cell viability, division, and morphogenesis at elevated temperatures.

Nucleotide binding is required for full septin function at 23°C. We used two genetic assays to determine if septin function is disrupted in mutant strains at 23°C. First, we assayed for synthetic phenotypes at 23°C in strains with mutations in the P-loops of two septins. In crosses of a $cdc11^{G32E}$ mutant with $cdc3^{K132E}$, $cdc3^{T133N}$, or $cdc12^{G44V}$ mutants, all single- and double-mutant segregants were obtained at the expected frequencies. However, all double-mutant segregants showed reduced viability and defects in cell division and morphogenesis (data not shown) (see Fig. S2K and L in the supplemental material). No viable $cdc11^{G32E}$ $cdc3^{G129V,\ K132E,\ T133N}$, $cdc11^{G32E}$ $cdc10^{K45T}$, or $cdc11^{G32E}$ $cdc12^{G44V,\ K47E,\ T48N}$ double mutant segregants were obtained, indicating synthetic lethality. Second, we assayed the phenotypes of septin, *cla4*Δ double-mutant strains at 23°C. *CLA4* encodes a PAK kinase involved in septin localization and function (14, 58), at least in part by direct phosphorylation of Cdc10p (75). At elevated temperatures, *cla4*Δ cells have defects in viability and septin localization, with septins often localizing to the tips of growing buds. However, at 23°C *cla4*Δ cells have only subtle defects in cell morphogenesis and septin localization (see Fig. S2B in the supplemental material) (58), with no defects in viability. All septin and *cla4*Δ single-mutant segregants were recovered at the expected frequencies. $cdc11^{D89A,\ G92}$ *cla4*Δ double-mutant segregants showed no synthetic phenotypes (see Fig. S2J in the supplemental material). $cdc11^{G32V}$ *cla4*Δ and $cdc11^{R35E}$ *cla4*Δ double-mutant segregants had reduced viability and synthetic defects in cell division and morphogenesis (see Fig. S2D and H in the supplemental material) (data not shown). $cdc11^{R35T}$ *cla4*Δ double-mutant segregants also showed synthetic phenotypes (see Fig. S2F in the supplemental material), indicating reduced function of $cdc11^{R35T}$. No viable $cdc3^{G129V,\ K132E,\ T133N}$ *cla4*Δ, $cdc10^{K45T}$ *cla4*Δ, $cdc11^{K172A,\ D174A}$ *cla4*Δ or $cdc12^{G44V,\ K47T,\ T48N}$ *cla4*Δ double-mutant segregants were obtained, indicating synthetic lethality. We conclude that mutations predicted to affect nucleotide binding have deleterious effects on septin function at 23°C.

Nucleotide binding is important for septin localization. Septin localization in yeast involves several steps (see the introduction), including localization to the cortex and formation of a cortical ring and then of a collar of filaments at the neck. To ask if nucleotide binding is important for septin localization, we localized functional Cdc3p-GFP or Cdc12p-GFP septins in wild-type and mutant cells before and during an 8-h shift to 37°C (see Fig. S1 in the supplemental material) (Table 2). As expected, after the shift to 37°C, septins were rapidly delocalized from the necks of *cdc12-6* mutant cells, which express a C-terminally truncated Cdc12p (58), and remained at the necks of wild-type and Ts^+ mutant cells. Septins remained at the necks of Ts cells that were arrested at S phase prior to the shift to 37°C. However, in cells progressing through the cell cycle, neck localization was gradually reduced in all Ts mutants, with most cells lacking neck-localized septins after 1 h exhibiting small buds (Table 2 and data not shown). These results suggest the mutants have a specific defect in septin localization during bud emergence.

To directly examine this possibility, wild-type and mutant strains were arrested in G_1 with α-factor at 23°C and septin localization was followed after release from cell cycle arrest at 37°C. As expected, in wild-type cells septins localized to the cell cortex and formed a collar at the neck of the new buds (Table 3; see also Movie S1 in the supplemental material). In Ts mutants, septins were unable to localize to a region on the cell cortex in the large majority of cells (Table 3; see also Movie S2 in the supplemental material), while in a minority of cells the septins localized to the tips of the buds. Similar results were obtained in mutant diploid cells released from hydroxyurea arrest at 37°C (data not shown). Our finding that septins are unable to localize to the cortex at restrictive temperature contrasts with the finding that septins localize to the cell cortex of most $cdc10^{S46N}$ $cdc12^{T48N}$ double-mutant cells at 37°C but are unable to form a collar at the neck, instead localizing to the bud tips (75). One possible explanation for these apparently

TABLE 2. Septin localization during log-phase growth and S-phase arrest

Strain	Relevant genotype	Temp (°C)	% Budded cells with septins at the neck[a]							
			At time (h) in log phase[b]						After hydroxyurea arrest at[c]:	
			0	1	2	3	5	8	0 min	90 min
M-2437	*CDC11*	23	99	99	99	96	96	95	ND	ND
M-2437	*CDC11*	37	99	94	99	99	90	91	99	100
M-2962	*cdc12-6*	37	91	1	0	0	0	0	96	4
M-2452	*cdc11*^{G32E}	37	100	50	24	5	5	3	93	96
M-2440	*cdc11*^{G32V}	37	99	77	29	23	12	5	91	94
M-2443	*cdc11*^{R35T}	37	99	96	94	95	94	90	99	98
M-2446	*cdc11*^{R35E}	37	99	95	82	38	29	14	96	95
M-2449	*cdc11*^{S36N}	37	97	94	60	53	27	11	ND	ND
M-3277	*cdc11*$^{D89A, G92A}$	37	96	93	92	93	90	89	ND	ND
M-3280	*cdc11*$^{K172A, D174A}$	37	92	31	12	1	0	0	ND	ND
M-2922	*CDC3*	37	92	93	87	87	85	86	90	87
M-2923	*cdc3*^{G129}	37	96	95	90	92	89	86	93	92
M-2927	*cdc3*$^{G129V, K132E, T133N}$	37	85	43	15	2	0	0	89	88
M-2855	*CDC10*	37	99	97	92	93	89	90	ND	ND
M-2856	*cdc10*^{G42V}	37	97	46	30	12	7	4	86	78
M-2857	*cdc10*^{K45T}	37	98	33	14	2	0	1	ND	ND
M-2863	*CDC12*	37	97	94	97	87	88	86	90	82
M-2864	*cdc12*^{G44V}	37	92	73	52	29	10	4	91	87
M-2865	*cdc12*^{K47T}	37	91	89	87	82	81	80	ND	ND
M-2866	*cdc12*$^{G44V, K47T, T48N}$	37	79	27	10	0	0	0	ND	ND
M-2867	*cdc12*$^{D98A, G101A}$	37	97	96	86	87	74	77	ND	ND

[a] Septin localization was determined by epifluorescence microscopy. More than 200 budded cells were counted per sample.
[b] The indicated strains were grown to mid-log phase at 23°C, and septin localization was determined before (0 h) and at the times indicated after shift to 37°C.
[c] Strains were grown to mid-log phase at 23°C and arrested with 0.2 M hydroxyurea, and septin localization was determined before and after 90 min at 37°C. ND, not determined.

contradictory results is that there is a range of septin behavior. Perhaps at semipermissive temperatures, nucleotide-binding mutant septins are able to localize to the cell cortex but are unable to form a collar. To test this hypothesis, we released nucleotide-binding mutant septin strains from cell cycle arrest at semipermissive temperatures. Under these conditions, septins localized to the cortex and then to the tips of the emerging buds in the majority of cells (Table 3; see also Movie S3 in the supplemental material). These data suggest that nucleotide binding is required for septins to localize to the cortex at restrictive temperature and that at semipermissive temperatures septins can localize to the cortex but are unable to form the collar.

Nucleotide binding is important for septin complex formation. To determine if nucleotide binding is important for septin-septin interactions, we first used the yeast two-hybrid system, which detects multiple interactions between wild-type septins (Table 4) (53). All mutant DBD- and AD-septin fusion proteins were expressed at wild-type levels, except for DBD-cdc3p$^{G129E, K132E, T133N}$, which was unstable and thus not assayed (data not shown). The cdc11p$^{D89A, G92A}$ G3-motif mutant and the cdc12p^{S43V} GTP hydrolysis-defective mutant proteins showed no defects in septin-septin interactions. In contrast, mutations that reduced septin function always reduced septin-septin interactions; mutations that affected septin function only at 37°C or in double mutant genetic analyses showed reduced septin-septin interactions (*cdc3*^{G129V}, *cdc3*^{K132T}, *cdc3*^{T133N}, *cdc11*^{R35T}, and *cdc12*^{G44V}) while mutations that resulted in inviability at 34°C or lower eliminated septin-septin interactions (*cdc10*^{K45T}, *cdc11*^{G32V}, *cdc11*$^{G32V, R35E, S36N}$, *cdc11*$^{K172A, K174A}$, and *cdc12*$^{G44V, K47E, T48N}$). Similarly, P-loop mutations can disrupt interactions of mammalian septins (8, 60). We noted that cdc11p^{R35E} and cdc11p^{S36N} retained the ability to interact with Cdc12p but not Cdc3p, Cdc10p, or Cdc11p, suggesting that Cdc11p and Cdc12p may interact directly.

Next, we used an in vitro assay to investigate the role of nucleotide binding on septin-septin interactions. Individual wild-type or mutant ^{35}S-labeled septins were expressed in rabbit reticulocyte lysate-coupled in vitro TnT mixtures, yielding proteins of the expected size that were recognized by the appropriate antibodies (Fig. 3A and data not shown). Equal amounts of individual septins were combined at 23°C and complexes isolated by immunoprecipitation or by binding a six-His-tagged septin to metal resin. As expected, wild-type septins formed an approximately stoichiometric complex (Fig. 3A). In pair-wise assays, the only interaction detected was between Cdc11p with Cdc12p, with the N-terminal regions of these proteins being sufficient for their interaction (Fig. 3A and C). In assays with three septins, Cdc3p bound the Cdc11p/Cdc12p complex, but with reduced stoichiometry (Fig. 3A). Cdc10p participated in complex formation only in the presence of the other three septins (Fig. 3A). In assays with mutant septins, full-length cdc11p^{R35T} interacted with Cdc12p at reduced levels and the N-terminal region of cdc11p^{R35T} was unable to interact with Cdc12p (Fig. 3B and C), confirming a modest effect of this mutation. All other full-length or N-terminal *cdc11p* mutant proteins tested were unable to bind Cdc12p (Fig. 3B and C). cdc12p nucleotide-binding mutant proteins were unable to bind Cdc11p (Fig. 3B, cdc12p^{G44V} and cdc12p$^{G44V, K47E, T48N}$), while loss of GTP hydrolysis did not affect the interaction with Cdc11p (Fig. 3B, cdc12p^{S43V}). In

TABLE 3. Septin localization after α-factor arrest and release[a]

Strain	Relevant genotype	Temp (°C)	Time (min)	% Budded cells	Septin localization (%)[b]			
					Neck	Absent	Tip	Other
M-2437	Wild type	37	0	3	100	0	0	0
			40	42	100	0	0	0
			80	81	99	1	0	0
		32	0	6	83	17	0	0
			40	52	100	0	0	0
			80	85	100	0	0	0
M-2927	*cdc3*$^{G129V,\ K132E,\ T133N}$	37	0	2	75	24	0	1
			40	78	5	73	22	0
			80	90	3	96	0	1
		30	0	2	100	0	0	0
			40	66	36	14	53	2
		80	93	54	40	3	3	
M-2857	*cdc10*^{K45T}	37	0	2	73	25	0	2
			40	78	3	81	14	2
			80	92	1	95	0	4
		32	0	4	78	22	0	0
			40	78	19	19	61	1
			80	83	28	57	11	4
M-2440	*cdc11*^{G32V}	37	0	2	75	25	0	0
			40	87	1	84	14	1
			80	97	0	98	0	2
		30	0	5	79	20	0	1
			40	70	17	31	52	0
			80	97	9	67	21	3
M-2866	*cdc12*$^{G44V,\ K47E,\ T48N}$	37	0	8	75	25	0	0
			40	80	3	88	8	1
			80	96	1	98	0	1
		30	0	11	86	12	2	0
			40	88	3	20	75	2
			80	94	1	95	2	2

[a] Strains were grown to mid-log phase in selective medium at 23°C, arrested with α-factor at 23°C, shifted to the temperature indicated for 20 min, and released into prewarmed medium lacking α-factor at the temperature indicated. Septin localization was determined by epifluorescence microscopy at the time indicated after release from α-factor arrest. Buds began emerging between 20 and 40 min after release from cell cycle arrest. At least 200 cells were counted per time point.

[b] The percentage of budded cells with septins localized to the neck as a collar, lacking localized septins, with septins at the tip of the bud, or with septins localized elsewhere (e.g., as a patch at the neck).

the presence of the three other wild-type septins, cdc3p$^{G129V,\ K132E,\ T133N}$ and cdc10p^{K45T} were unable to participate in complex formation and, in all cases, a nucleotide-binding mutant septin did not participate in or disrupt complex formation when mixed with the four wild-type septins (data not shown).

We then used a coimmunoprecipitation approach to determine if nucleotide binding is involved in septin-septin interactions in vivo. Wild-type and mutant strains were grown to mid-log phase at 23°C, and the culture was divided, with one-half shifted to 37°C for 2 h. All wild-type and mutant septins were expressed at similar levels at 23°C and after temperature shift (Fig. 4 and data not shown). Septin complexes were isolated by immunoprecipitation and detected by immunoblotting. A complex of Cdc3p, Cdc10p, Cdc11p, and Cdc12p was efficiently isolated from wild-type strains at 23°C or 37°C (Fig. 4). Complexes were also isolated from all mutants at 23°C (data not shown) and from Ts$^+$ mutants at 37°C (Fig. 4A and B, *cdc11*^{R35T}, *cdc3*^{K132E}, *cdc11*$^{D89A,\ G92A}$, and *cdc12*$^{D98A,\ G101A}$). In Ts mutant strains at 37°C, the mutant septin was absent, or present at greatly reduced levels, in the complexes (Fig. 4A and B, *cdc10*^{K45T}, *cdc11*^{G32E}, *cdc11*^{G32V}, *cdc11*^{R35E}, *cdc11*$^{G32E,\ R35E,\ S36N}$, *cdc11*$^{K172A,\ D174A}$, *cdc12*^{G44V}, *cdc12*$^{G44V,\ K47E,\ T48N}$, and *cdc3*$^{G129V,\ K132E,\ T133N}$). In Ts mutant strains at semipermissive temperatures, both complete and partial septin complexes were present (Fig. 4C).

Although the qualitative coimmunoprecipitation (IP) analyses did not detect a clear defect in the interactions of nucleotide-binding mutant septins at 23°C in vivo, the two-hybrid and in vitro binding assays and the double mutant genetic analyses suggested that mutant septins have reduced function at 23°C. One possibility is that the defects in septin-septin interactions in vivo are mild at 23°C and not detectable by qualitative assays. To test this idea, we first used a quantitative coimmunoprecipitation assay. For five independent experiments, wild-type and *cdc11* mutant strains were grown to mid-log phase at 23°C. Septin complexes were immunoprecipitated with anti-Cdc3p antibodies, and the ratio of Cdc3p to the coimmunoprecipitated wild-type or mutant Cdc11p was determined by immunoblotting. Compared to wild-type Cdc11p, there was a reproducible reduction in the amount of coimmunoprecipitated cdc11p mutant proteins: cdc11p^{R35T} (0.92 ±

TABLE 4. Two-hybrid interactions among *S. cerevisiae* wild-type and mutant septins

DBD fusion	β-Galactosidase activity with DBD fusion[a]															
	pJG4-5	*CDC3*	*CDC3-N*	*CDC3-C*	*CDC10*	*CDC11*	*CDC11-N*	*CDC11-C*	*cdc11G32V*	*cdc11R35T*	*cdc11R35E*	*cdc11S36N*	*cdc113nt*	*CDC12*	*CDC12-N*	*CDC12-C*
None[b]	12	12	3	4	10	6	17	14	15	10	13	8	31	12	10	5
CDC3	15	28	2	21	26	**2,803**	**150**	7	10	**931**	8	8	5	**1,942**	**618**	8
cdc3G129V	8	11	6	19	16	**361**	**112**	7	5	**101**	13	5	6	**635**	**235**	15
cdc3K132T	19	23	23	18	43	**869**	**178**	27	19	**366**	41	31	41	**1,084**	**311**	43
cdc3T133N	6	18	37	35	13	**663**	**148**	4	14	**215**	32	15	15	**1,160**	**205**	23
CDC3-N	17	8	2	12	**156**	**227**	50	21	7	44	9	9	38	**249**	**651**	15
CDC3-C	14	20	5	4	27	54	82	3	15	52	40	41	6	**1,853**	29	**201**
CDC10	10	**486**	**109**	4	11	**1,708**	**366**	29	10	**953**	23	97	10	**333**	41	22
cdc10K45T	21	28	27	ND	ND	18	12	ND	21	16	38	ND	ND	30	40	ND
CDC11	19	11	2	3	40	**2,192**	60	5	9	**1,421**	7	10	9	**1,381**	**1,843**	6
CDC11-N	4	15	5	16	34	**2,092**	**2,383**	10	24	**1,976**	4	14	20	**1,440**	**1,124**	9
CDC11-C	3	14	14	14	7	13	51	28	30	4	1	9	5	15	15	10
cdc11G32V	5	2	2	14	10	14	10	14	5	2	2	4	3	16	15	13
cdc11R35T	8	15	10	16	38	**2,104**	52	8	9	**836**	10	35	7	**1,052**	**717**	7
cdc11R35E	7	15	5	11	7	37	5	10	12	6	8	8	8	**695**	**719**	8
cdc11S36N	4	14	6	11	15	13	3	6	6	7	6	11	10	**1,129**	**994**	7
cdc11 3nt	6	21	14	27	9	36	11	6	19	7	9	46	13	16	3	4
cdc11 G3	11	9	ND	ND	65	**2,306**	**125**	4	ND	ND	ND	ND	ND	**2,021**	**2,357**	5
cdc11 G4	10	23	ND	ND	11	13	8	16	ND	ND	ND	ND	ND	7	11	8
CDC12	7	**157**	5	63	15	**2,568**	**954**	11	10	**1,820**	**654**	**1,622**	10	**2,784**	77	7
CDC12-N	5	14	15	18	45	**2,925**	**527**	44	21	**525**	**128**	78	10	**439**	**196**	11
CDC12-C	7	**211**	10	**389**	26	16	40	7	6	5	2	48	8	**1,538**	77	**138**
cdc12G44V	6	**121**	ND	ND	14	**852**	**311**	5	ND	ND	ND	ND	ND	**666**	ND	ND
cdc12 3nt	4	14	ND	ND	7	12	7	10	ND	ND	ND	ND	ND	9	ND	ND
cdc12S43V	11	**184**	ND	ND	19	**1,986**	**753**	ND	ND	ND	ND	ND	ND	**2,480**	ND	ND

[a] Two-hybrid assays were performed as described in Materials and Methods. At least four independent β-galactosidase assays were done for each combination. Strains were grown at 23°C for 16 h in minimal medium containing leucine and 1% raffinose and 2% galactose. Shown are the average values in Miller units. Values above 100 and at least ninefold higher than the corresponding control (pEG202 with no insert) were deemed positive and are shown in boldface. -N and -C indicate the N- and C-terminal fragments, respectively, of the indicated gene (16). *cdc11 G3* is $cdc11^{D89A,\ G92A}$, *cdc11 G4* is $cdc11^{K172A,\ D174A}$, *cdc11 3nt* is $cdc11^{G32V,\ R35E,\ S36N}$, and *cdc12 3nt* is $cdc12^{G44V,\ K47E,\ T48N}$. ND, not done.

[b] pEG202 with no insert.

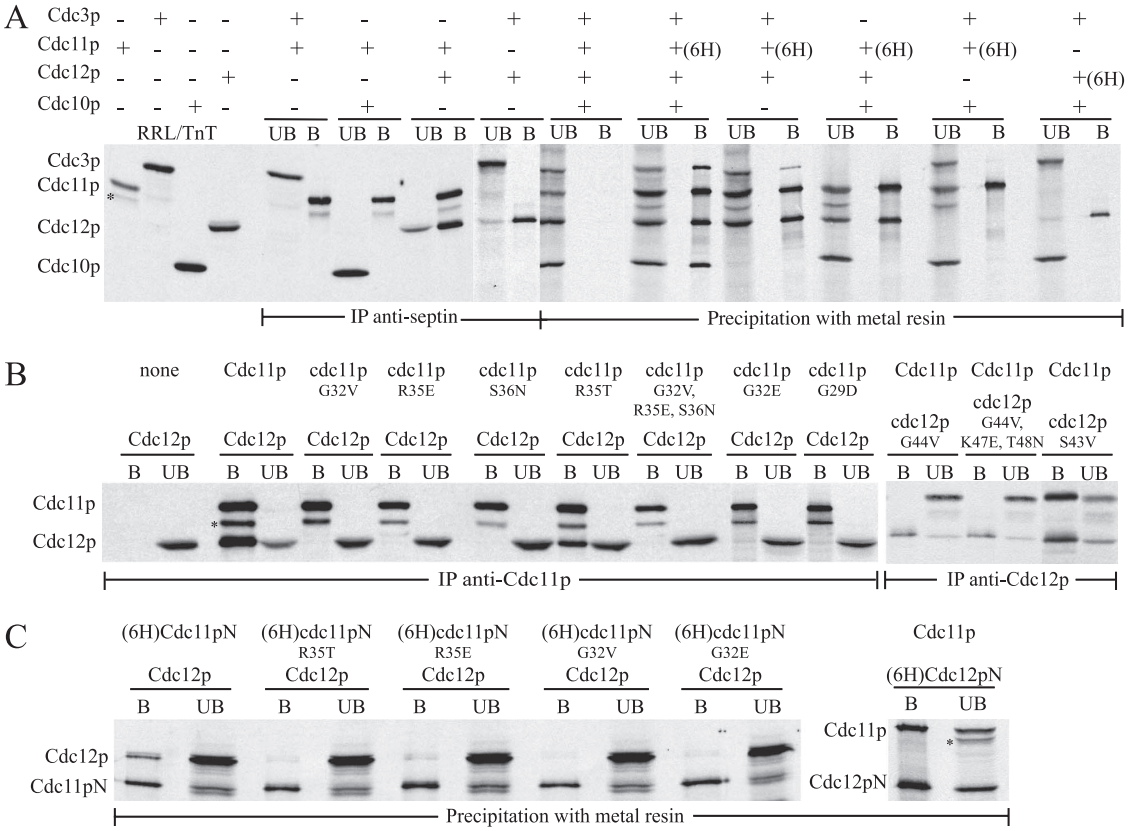

FIG. 3. Analysis of direct septin interactions and the role of GTP binding in septin complex formation in vitro. ^{35}S-labeled septins made individually by coupled in vitro transcription and translation were incubated together at 23°C for 1 h, and complexes were isolated by immunoprecipitation or binding to metal resin, as indicated. Septins in the unbound (UB) and bound (B) fractions were detected by autoradiography. The asterisk indicates a nonspecific band from the Cdc11p synthesis. "(6H)" indicates the presence of six N-terminal histidines. (A) Individual expression of Cdc3p, Cdc10p, Cdc11p, and Cdc12p and interactions among wild-type septins. For combinations of two septins, complexes were immunoprecipitated using anti-Cdc11p antibodies or, for the Cdc3p/Cdc12p pair, anti-Cdc12p antibodies. (B) Effects of P-loop mutations on the pair-wise interaction of full-length Cdc11p and Cdc12p. (C) Interaction of the N-terminal regions of Cdc11p and Cdc12p and the effects of mutations in the Cdc11p P-loop. Cdc11pN, residues 1 to 295; Cdc12pN, residues 1 to 311.

20); cdc11p^{G32V}, (0.77 ± 0.20); cdc11p^{G32E}, (0.74 ± 0.26); cdc11p^{R35E} (0.79 ± 0.21), and cdc11p$^{G32V, R35E, S36N}$ (0.71 ± 0.17). Next, we used an in vivo competition assay for neck localization. We reasoned that if a mutation results in a reduced ability to participate in septin complexes the mutant septin would be an ineffective competitor with a wild-type septin for neck localization. In control experiments, Cdc11p was detected at over 99% of necks using anti-Cdc11p antibodies, and an HA-tagged Cdc11p was detected at over 95% of necks in the presence of untagged, wild-type Cdc11p competitor (Fig. 5A). At 23°C, cdc11p$^{G32E-3HA}$ localized efficiently to the neck in the presence of untagged cdc11p^{G32E} but was effectively competed by wild-type Cdc11p (Fig. 5A). Similarly, after 2 h at 37°C, cdc11p$^{G32E-3HA}$ competed efficiently with cdc11p^{G32E} but not with Cdc11p (Fig. 5A). We also quantitatively assayed the efficiency of neck localization of wild-type and mutant YFP-tagged septins. At 23°C, a cdc11p G4 motif mutant protein localized efficiently to the neck in the absence, but not the presence, of wild-type Cdc11p (Fig. 5B, cdc11p$^{K172A, K174A}$). cdc3p and cdc12p P-loop mutant proteins were also ineffective competitors for neck localization (Fig. 5B, cdc3p$^{G129V, K132E, T133N}$ and cdc12p$^{G44V, K47E, T48N}$). Although cdc10p^{K45T} competed effectively at 23°C, it was unable to localize to the neck efficiently in the presence of wild-type Cdc10p at 27°C (Fig. 5B), a temperature at which the *cdc10^{K45T}* strain shows full viability and normal septin localization (data not shown). Together, these results indicate that nucleotide binding is important for full septin-septin interactions at 23°C and is essential for septin-septin interactions at elevated temperatures.

Our results also provide information on septin-septin interactions in vivo. In agreement with the remaining three septins interacting in *cdc10*Δ and *cdc11*Δ cells at 23°C (22), the remaining three septins interacted in Ts *cdc10* and *cdc11* mutant strains at 37°C (Fig. 4A, *cdc11^{G32E}*, anti-Cdc12p IP, and B, *cdc10^{K45T}*, anti-Cdc11p, -Cdc12p, and -Cdc3p IPs). In agreement with our in vitro binding results, Cdc11p and Cdc12p can interact in the absence of Cdc3p and Cdc10p (Fig. 4A, *cdc11^{R35E}*, anti-Cdc11p IP), while Cdc11p does not participate in complex formation in the absence of Cdc12p (Fig. 4B, *cdc12$^{G44V, K47E, T48N}$*, anti-Cdc11p and -Cdc12p IPs). The association of Cdc10p with the complex appears to require Cdc3p, as a decrease of Cdc3p results in a concomitant decrease in Cdc10p (Fig. 4A, *cdc3$^{G129V, K132E, T133N}$*, anti-Cdc11p

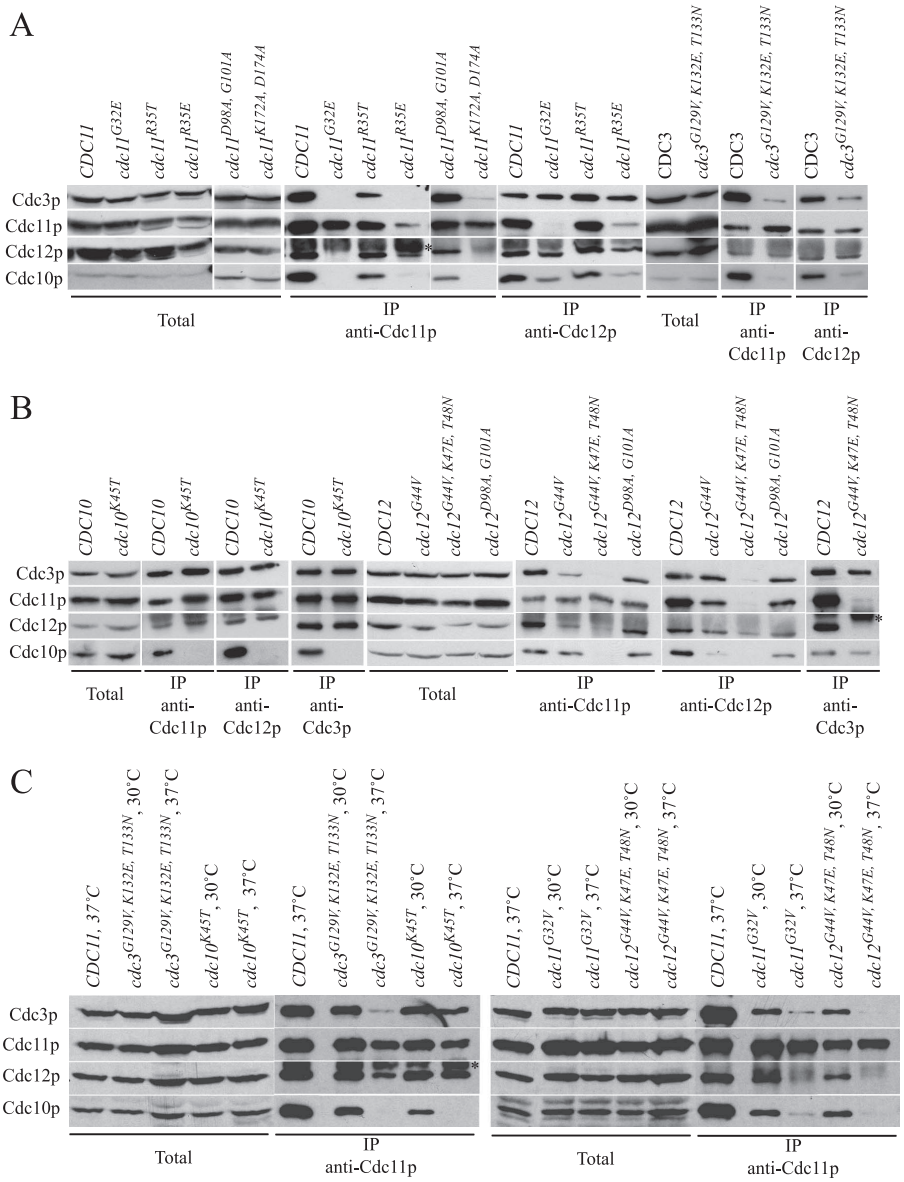

FIG. 4. Analysis of septin complexes in wild-type and mutant strains. (A and B) Septin complexes are disrupted at 37°C in GTP-binding mutants. Strains were grown to mid-log phase at 23°C and shifted to 37°C for 2 h. Lysates from wild-type and *cdc11* or *cdc3* mutant strains (A) or *cdc10* or *cdc12* mutant strains (B) were prepared, and total protein, or immunoprecipitates obtained with the indicated antibodies, were separated by SDS-PAGE and immunoblotted to detect Cdc3p, Cdc10p, Cdc11p, or Cdc12p. Strains are as described for Fig. 1, with M-2332 used as the wild-type strain. The asterisk indicates the immunoglobulin heavy chain, which migrates just above Cdc12p. (C) Septin complexes are partially disrupted at semipermissive temperatures. *MAT***a** strains were arrested with α-factor at 23°C, shifted to the indicated temperature for 20 min, and released from cell cycle arrest at the indicated temperature. At 40 min after release, lysates were prepared and septin complex formation assayed as described above. Strains are as for Fig. 1, with M-2332 used as the wild-type strain.

and -Cdc12p IPs). In contrast to our in vitro binding data, Cdc3p and Cdc10p can interact with each other in vivo in the absence of Cdc11p and Cdc12p (Fig. 4B, $cdc12^{G44V,\ K47E,\ T48N}$, anti-Cdc3p IP) and Cdc12p can interact with Cdc3p and Cdc10p in the absence of Cdc11p (Fig. 4A, $cdc11^{G32E}$, anti-Cdc12p IP). It is possible these latter interactions are enhanced in vivo by posttranslational modifications.

Lack of evidence for septin nucleotide-binding in the function of septin-associated proteins. A major role of yeast septins is to serve as a scaffold to direct the localization of septin-associated proteins to the neck (reviewed in references 28 and 55). In all cases, the function of septin-associated proteins requires their septin-dependent localization to the neck. To determine if nucleotide binding is required for their interactions with septin-associated proteins, we investigated the effects of nucleotide binding mutations on the function of septin-associated proteins (Table 5). As our results suggested nucleotide binding is reduced or absent in the mutants at 23°C, these assays were done at 23°C to avoid loss of function simply due to lack of neck-localized septins. In the mutant strains,

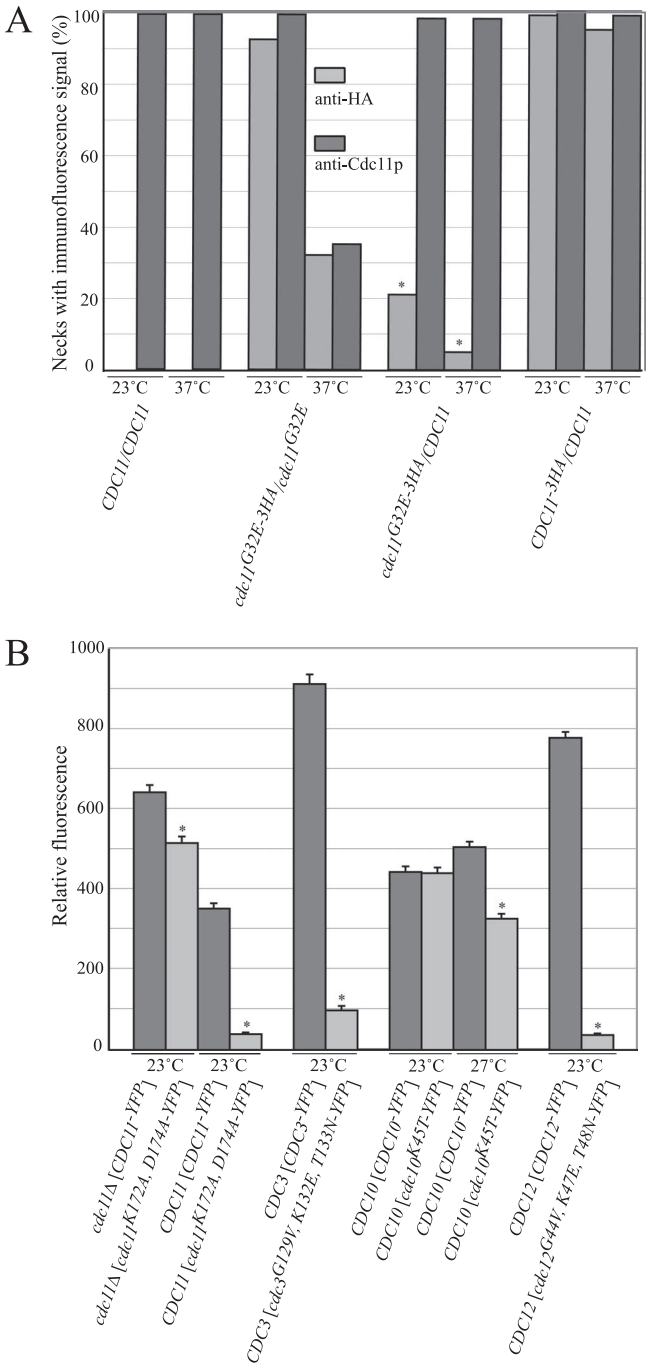

FIG. 5. In vivo competition assay of nucleotide-binding mutant septins for neck localization. (A) Strains YEF473 (*CDC11*/*CDC11*), M-2630 (*cdc11*$^{G32E\text{-}3HA}$/*cdc11*^{G32E}), M-2634 (*cdc11*$^{G32E\text{-}3HA}$/*CDC11*), and M-2633 (*CDC11-3HA*/*CDC11*) were grown to mid-log phase in YM-P medium at 23°C and processed for immunofluorescence with anti-HA and anti-Cdc11p antibodies before, or after, a 2-h shift to 37°C. More than 200 budded cells were counted for each sample. Asterisks indicate that means of the 37°C sample were significantly different from the mean of the corresponding 23°C sample (two-tailed Student's *t* test; $P < 0.005$). (B) YEF473A carrying low-copy-number plasmids expressing the indicated YFP-tagged septin was grown to mid-log phase in selective medium at 23° or 27°C, as indicated. Cells with medium buds were observed by fluorescence microscopy, and the YFP signal from the necks of over 200 cells was quantitated for each strain, as described in Materials and Methods. Bars indicate standard errors. Asterisks indicate means significantly different from the mean of the strain expressing the corresponding wild-type septin (two-tailed Student's *t* test; $P < 0.005$).

cells formed normal shmoos in response to mating pheromone with septins properly localized at the base. Chitin was properly deposited in the cell wall at the base of the shmoo and on the mother-side of the neck of budded cells, indicating normal localization and function of the chitin synthase III complex. Axial and bipolar bud site selection were normal, indicating proper localization and function of the bud site selection proteins. Cytokinesis and cell separation were normal, indicating proper function of the actomyosin contractile ring, synthesis of the septum, and localized secretion of chitinases at the neck. Finally, cell morphology was normal, indicating proper function of the Hsl1p, Hsl7, and Swe1p cell cycle regulatory complex and in secretion targeted to the base of the bud (25, 58). Together, these results do not provide any evidence that septin nucleotide binding is specifically required for the localization or activation of septin-associated proteins.

DISCUSSION

In this study, we addressed the role of nucleotide binding by the *S. cerevisiae* Cdc3p, Cdc10p, Cdc11p, and Cdc12p septins. We found that these septins all bind GTP and that the P-loop and G4 motifs, but not the G3 motif, are important for nucleotide binding. The major finding of this work is that nucleotide binding has a conserved role in septin-septin interactions and, therefore, in septin complex formation. Our studies also suggest that septins are localized to the cell cortex as preformed complexes and support a model in which assembly into filaments is important for formation of the septin collar. Finally, our studies provide insight into the order of the yeast septins in the linear core complex.

Cdc3p, Cdc10p, Cdc11p, and Cdc12p are GTP-binding proteins. Previous studies yielded conflicting results as to whether or not Cdc3p, Cdc10p, Cdc11p, and Cdc12p all bind GTP (see introduction). Our results provide strong evidence that each of these septins binds GTP, in agreement with the findings of two previous studies (19, 76), and we showed that the conserved P-loop and G4 motifs are important for GTP binding. That all four septins bind GTP is also suggested by the similar phenotypes of *cdc3*, *cdc10*, *cdc11*, and *cdc12* nucleotide-binding mutant strains, as discussed further below. Surprisingly, we found no role for the G3 motif in septin GTP binding or function. Perhaps in septins this motif is involved in nucleotide hydrolysis, as it is in dynamin and AAA ATPases (4, 35, 59). However, as GTP hydrolysis is not required for the formation of septin complexes or filaments (19, 21, 49, 70) or known aspects of septin function in yeast (75), the role of GTP hydrolysis remains enigmatic.

We can provide two possible explanations for the lack of a previous study to detect GTP binding by bacterially expressed Cdc3p and Cdc11p in vitro (75). First, yeast and metazoan septins expressed individually in *E. coli* are free of bound nucleotide and largely insoluble (our unpublished results and references 19, 37, and 69), suggesting they are not properly folded. Perhaps *E. coli*-expressed Cdc10p and Cdc12p more readily bind nucleotide from this nonphysiological state than do Cdc3p or Cdc11p. Also, as GTP binding by septins in vitro is typically slow and inefficient, especially with nucleotide-free, *E. coli*-expressed septins (23, 62, 69, 75, 76), the GTP-binding activity of *E. coli*-expressed Cdc3p and Cdc11p may have sim-

TABLE 5. Function of wild-type and mutant septins in septin-dependent events[a]

Relevant genotype	Bud site selection[b]		Chitin deposition[c]	Shmoo		Cell separation/ cytokinesis[f]	Cell morphology[g]	Diploid strain	Haploid strain
	Axial	Bipolar		Formation[d]	Localization[e]				
*rsr1*Δ	4	3	ND	ND	ND	ND	ND	LSY388	LSY365
*bud9*Δ	ND	6	ND	ND	ND	ND	ND	HH615	
CDC3	97	ND	96	92	93	96	97		M-2922
cdc3^{G129V}	98	ND	97	94	91	95	97		M-2923
cdc3^{K132T}	97	ND	97	98	94	94	96		M-2924
cdc3^{K132E}	97	ND	94	93	89	94	98		M-2925
cdc3^{T133N}	99	ND	95	91	91	96	98		M-2926
cdc3$^{G129V,\ K132E,\ T133N}$	95	90	94	90	87	91	93	M-3474	M-2927
*cdc10*Δ[h]	ND	ND	ND	ND	ND	73	57		M-2894
CDC10	98	ND	91	94	94	98	98		M-2855
cdc10^{G42V}	96	ND	89	95	92	97	96		M-2856
cdc10^{K45T}	98	ND	93	91	94	97	97		M-2857
*cdc11*Δ[h]	ND	ND	ND	ND	ND	5	2		M-2897
CDC11	94	91	99	88	94	99	99	M-2334	M-2437
cdc11^{G29D}	98	ND	95	95	97	99	98		M-2859
cdc11^{G32E}	95	92	98	ND	88	98	98	M-2344	M-2452
cdc11^{G32V}	98	87	99	90	80	98	94	M-2325	M-2440
cdc11^{R35T}	98	90	99	89	94	99	98	M-2313	M-2443
cdc11^{R35E}	98	84	98	90	93	99	99	M-2301	M-2446
cdc11^{S36N}	99	91	99	96	90	99	96	M-2307	M-2449
cdc11$^{G32V,\ R35E,\ S36N}$	99	91	97	93	98	99	95	M-3473	M-2860
cdc11$^{D89A,\ G92A}$	99	93	98	92	98	97	99	M-3186	M-3277
cdc11$^{K172A,\ D174A}$	97	ND	97	90	75	91	91		M-3280
CDC12	93	ND	94	95	91	96	97		M-2863
cdc12^{G44V}	95	ND	95	94	95	96	94		M-2864
cdc12^{K47T}	94	ND	95	91	91	98	95		M-2865
cdc12$^{G44V,\ K47E,\ T48N}$	90	ND	90	95	77	91	83		M-2866
cdc12$^{D98A,\ G101A}$	95	ND	95	86	92	96	92		M-2867

[a] All assays used the indicated haploid strains, except for analysis of bipolar budding, which used the indicated diploid strains. Strains were grown in selective medium at 23°C. Shown is the percentage of cells with wild-type function or localization ($n > 200$).
[b] Scoring of axial and bipolar budding is described in Materials and Methods.
[c] Chitin deposited asymmetrically to the mother-side of the neck of budded cells.
[d] Shmoos (mating projections) present after 4 h exposure to α-factor.
[e] Septins and chitin localized to the base of the mating projection.
[f] Complete cytokinesis and cell separation, as determined by the percentage of cells with one or two cell bodies following 5 s of mild sonication.
[g] Cell morphology was scored as described elsewhere (56), with buds scored as elongated if the length of the bud was more than twice the width of the mother cell.
[h] Chitin is poorly localized in *cdc10*Δ (15) and *cdc11*Δ cells (unpublished observations), precluding accurate scoring of bud site selection.

ply been below the detection limit of the assays used by Versele and Thorner (75).

Nucleotide binding has a conserved role in septin-septin interactions and complex formation. Several possible functions for septin nucleotide binding have been proposed (reviewed in references 20, 28, and 55). First, nucleotide binding may be important in septin-septin interactions and complex formation. Second, it may be specifically involved in the assembly of filaments from septin complexes, as suggested by the finding that P-loop mutant Cdc10p and Cdc12p proteins formed apparently normal complexes but were unable to form filaments in vitro (75). Finally, nucleotide binding, or the status of the bound nucleotide, may be involved in septins interacting with, or regulating the activity of, septin-associated proteins. To investigate the function of septin nucleotide binding, we assessed the effects of P-loop, G3, and G4 motif mutations on septin function.

We found that *cdc3*, *cdc10*, *cdc11*, and *cdc12* P-loop mutant strains and a *cdc11* G4 motif mutant strain were temperature sensitive for cell viability, morphogenesis, and division and that there was an excellent correlation between the defects in nucleotide binding and septin function. Temperature-sensitive defects in septin function were noted previously for *cdc10* and *cdc12* P-loop mutant strains (75). Although single mutant strains displayed no phenotypes at 23°C, double mutant genetic analyses indicated that P-loop and G4 motif mutant septins are compromised for function at this temperature. These results indicate nucleotide binding is important for septin function at all temperatures and that the temperature sensitivity of the mutant strains is due, at least in part, to temperature-sensitive redundancy of function for septin GTP binding.

We found that mutations in the septin P-loop or G4 motif mutations reduced or eliminated septin-septin interactions in two-hybrid and in vitro binding assays while mutations in the G3 motif or mutations that reduced GTP hydrolysis had no effect. Coimmunoprecipitation and competition assays for neck localization confirmed that P-loop and G4 motif mutations reduced septin-septin interactions at 23°C in vivo and strongly reduced, or eliminated, interactions at 37°C. The extent of the defects in interaction paralleled the extent of the defects in GTP binding and viability. Together, these results indicate that the primary role of nucleotide binding is in septin-septin interactions and formation of the hetero-oligomeric complex, and the findings are most consistent with nucleotide binding having a structural role. Our data do not support the conclusion of a previous study that nucleotide binding is not

important for septin-septin interactions (75). Because of the conservation of septin nucleotide binding and formation of hetero-oligomeric complexes, it is likely that the role of nucleotide binding in septin complex formation is conserved.

Nucleotide binding does not appear essential for septin-septin interactions under all conditions. Although nucleotide-free, yeast septins purified after individual expression in *E. coli* show specific interactions in in vitro binding assays (our unpublished results and references 74 and 75) and at 23°C all mutant septins that we generated were able to at least partially participate in septin complexes in vivo. However, as wild-type septins do not appear to exist in a nucleotide-free state in vivo, these interactions are unlikely to be of physiological relevance.

We can provide several explanations for why a previous study did not detect an effect of Cdc10p or Cdc12p P-loop mutations on septin-septin interactions (75). First, although no qualitative defects in complex formation were found by immunoprecipitation from a *cdc12*^{T48N} mutant strain at 37°C, this mutation has only modest affect on septin function, suggesting it has modest defects in interaction that would only be detected by quantitative analyses. (Septin-septin interactions in the *cdc10*^{S46N} *cdc12*^{T48N} double mutant strain, which is inviable at 37°C, were not examined.) Second, although P-loop mutations in *E. coli*-expressed Cdc10p or Cdc12p did not qualitatively reduce septin-septin interactions in vitro, the ability of nucleotide-free septins to interact, combined with the high concentrations of septins used in these assays, may have masked any defects in interaction. If the mutant septins were incorporated into complexes at substoichiometric levels, as our data suggest, the resulting partial complexes would lead to the observed defects in filament assembly (19, 22, 74).

Another possible, nonexclusive role for septin nucleotide binding is in providing spatial or temporal regulation to septins binding to septin-associated proteins or regulating their activity (reviewed in references 28, 46, and 64). Studies of mammalian septins are consistent with such a role. The ARTS septin promotes apoptosis by binding and inactivating XIAP, an inhibitor of apoptosis, and mutation of the ARTS P-loop prevents this interaction and its proapototic function (30). Sept2 binds the GLAST astrocyte glutamate transporter and Sept5 binds the syntaxin t-SNARE, and these interactions are most robust with nucleotide-free or GDP-bound septins. Overexpression of Sept2 or Sept5 P-loop mutants, but not of wild-type septins, inhibits GLAST activity and secretion, respectively (6, 50). However, that septin-nucleotide-binding status affects septin function under physiological conditions has not yet been demonstrated. In yeast, we found no defects in the function of septin-associated proteins in septin nucleotide-binding mutant strains with properly localized septins, providing no support for such a role of nucleotide binding in septin function in yeast.

The role of complexes in septin localization. Using the nucleotide-binding mutant strains, we investigated the role of complexes in septin localization. We found that in the absence of complete septin complexes, septins were unable to localize to a region of the cortex in late G_1. The only other mutants described that share this phenotype are loss-of-function mutations in *cdc42*, *cdc24* (*CDC24* encodes a GEF for Cdc42p) and in haploid *gic1*Δ *gic2*Δ cells at restrictive temperature (40). Recent work indicates that Cdc42p-GTP dependent localization of septins to the cell cortex involves interactions of septins with the Gic1p/Gic2p Cdc42p effector proteins and with components of an uncharacterized, redundant pathway (40). Borg3, an effector protein for the mammalian Cdc42p GTPase, also binds preassembled complexes of Sept2/Sept6/Sept7 but not septin monomers (69). Together, these results indicate that Cdc42p-dependent factors interact with complete septin complexes but not with incomplete complexes or septin monomers. An attractive feature of this model is that it provides a mechanism of quality control, preventing the cortical localization of partial septin complexes or monomers that could have detrimental affects, perhaps by inhibiting filament assembly.

The next stages of septin localization are the formation of a well-defined cortical ring with rapidly exchanging septin subunits and the maturation of this ring into a collar of filaments with nondynamic subunits. In *cdc3*, *cdc10*, *cdc11*, and *cdc12* nucleotide-binding mutant strains at semipermissive temperatures, we found that septins formed both complete and partial complexes and localized to the cortex in late G_1 but were unable to form a collar, instead localizing to the tips of the emerging buds as seen previously with *cdc10* and *cdc12* P-loop mutant strains (75). A similar pattern of septin localization to bud tips in the absence of collar formation is observed in strains with reduced GTP-hydrolysis by Cdc42p (11, 26) or at 30°C in strains lacking the Elm1p or Cla4p kinases, suggesting a role for Cdc42p GTP hydrolysis and septin phosphorylation in the release of septins from the cortical localization factors or in the assembly of septin filaments (25, 26). We suggest that the reduced amount of complete septin complexes in the mutant strains at semipermissive temperatures is insufficient to support filament assembly and that, in the absence of filament assembly, the septins are unable to form the collar, instead interacting with factors at the tip of the bud.

Organization of *S. cerevisiae* septin complexes. Recent studies suggest that septin complexes consist of a linear assembly of two (*Caenorhabditis elegans*), three (mammalian), or four (*S. cerevisiae*) septins. These complexes interact head-to-head, forming nonpolar core complexes containing two of each septin, with filaments assembled by end-to-end association of core complexes (42, 70). By a combination of two-hybrid and in vitro binding assays and coimmunoprecipitations from mutant strains, we find that Cdc11p and Cdc12p and that Cdc3p and Cdc10p can form bimolecular complexes. Cdc3p can interact with Cdc11p/Cdc12p in the absence of Cdc10p, and Cdc10p cannot interact with Cdc11p/Cdc12p in the absence of Cdc3p. These results are largely consistent with interactions of *E. coli*-expressed septins (74) and indicate that the order of *S. cerevisiae* septins in the linear complex is Cdc10p-Cdc3p-Cdc12p-Cdc11p. A similar organization is consistent with in vivo interaction results of the orthologous *Schizosaccharomyces pombe* septins [Spn2p (Cdc10p)-Spn1(Cdc3p)-Spn4(Cdc12p)-Spn3(Cdc11p)] (2). Our results do not allow us to determine if the octomeric core complex is generated by head-to-head interactions of Cdc11p (Cdc10p-Cdc3p-Cdc12p-Cdc11p/Cdc11p-Cdc12p-Cdc3p-Cdc10p) or Cdc10p (Cdc11p-Cdc12p-Cdc3p-Cdc10p/Cdc10p-Cdc3p-Cdc12p-Cdc11p).

ACKNOWLEDGMENTS

We thank John Pringle for strains and plasmids, Erfei Bi and Jamie Konopka for plasmids, Erfei Bi, Christine Field, Alina Vriabioui, and Jeremy Thorner for valuable discussions and communication of unpublished results, Dave Sept and Xiange Zheng for help with the molecular modeling, John Cooper for generous sharing of space and resources, and members of the Cooper lab for valuable discussions. We thank Bob Matts for reagents and help with the TnT assays.

This work was supported by National Institutes of Health grant RO1GM62392 to M.L.

ADDENDUM IN PROOF

Bertin et al. recently presented evidence suggesting that the yeast septin core complex consists of an octomer of Cdc11p-Cdc12p-Cdc3p-Cdc10p/Cdc10p-Cdc3p-Cdc12p-Cdc11p (A. Bertin, M. McMurray, P. Grob, S. Park, G. Garcia III, I. Patanwala, H. Ng, T. Alber, J. Thorner, and E. Nogales, Proc. Natl. Acad. Sci. USA **105:**8274–8279, 2008).

REFERENCES

1. **Adams, A. E., and J. R. Pringle.** 1984. Relationship of actin and tubulin distribution to bud growth in wild-type and morphogenetic-mutant *Saccharomyces cerevisiae* J. Cell Biol. **98:**934–945.
2. **An, H. A., J. L. Morrell, J. L. Jennings, A. J. Link, and K. L. Gould.** 2004. Requirements of fission yeast septins for complex formation, localization, and function. Mol. Biol. Cell **15:**5551–5564.
3. **Ausubel, F. M., R. Brent, R. E. Kingston, D. D. Moore, J. G. Seidman, J. A. Smith, and K. Struhl.** 1998. Current protocols in molecular biology. John Wiley and Sons, New York, NY.
4. **Babst, M., B. Wendland, E. J. Estepa, and S. D. Emr.** 1998. The Vps4p AAA ATPase regulates membrane association of a Vps protein complex required for normal endosome function. EMBO J. **17:**2982–2993.
5. **Beites, C. L., K. A. Campbell, and W. S. Trimble.** 2005. The septin Sept5/CDCrel-1 competes with *a*-SNAP for binding to the SNARE complex. Biochem. J. **385:**347–353.
6. **Beites, C. L., H. Xie, R. Bowser, and W. S. Trimble.** 1999. The septin CDCrel-1 binds syntaxin and inhibits exocytosis. Nat. Neurosci. **2:**434–439.
7. **Bi, E., and J. R. Pringle.** 1996. *ZDS1* and *ZDS2*, genes whose products may regulate Cdc42p in *Saccharomyces cerevisiae*. Mol. Cell. Biol. **16:**5264–5275.
8. **Blaser, S., S. Roseler, H. Rempp, H. Bartsch, H. Bauer, M. Lieber, E. Lessmann, L. Weingarten, A. Busse, M. Huber, and B. Zieger.** 2006. Human endothelial cell septins: SEPT11 is an interaction partner of SEPT5. J. Pathol. **210:**103–110.
9. **Brakoulias, A., and R. M. Jackson.** 2004. Towards a structural classification of phosphate binding sites in protein-nucleotide complexes: an automated all-against-all structural comparison using geometric matching. Proteins **56:**250–260.
10. **Castillon, G. A., N. R. Adames, C. H. Rosello, H. S. Seidel, M. S. Longtine, J. A. Cooper, and R. Heil-Chapdelaine.** 2003. Septins have a dual role in controlling mitotic exit in budding yeast. Curr. Biol. **13:**654–658.
11. **Caviston, J. P., M. Longtine, J. R. Pringle, and E. Bi.** 2003. The role of Cdc42p GTPase-activating proteins in assembly of the septin ring in yeast. Mol. Biol. Cell **14:**4051–4066.
12. **Colicelli, J.** 2004. Human RAS superfamily proteins and related GTPases. Science STKE **250:**rel13.
13. **Combet, C., C. Blanchet, C. Geourjon, and G. Deléage.** 2000. NPS@: network protein sequence analysis. Trends Biochem. Sci. **25:**147–150.
14. **Cvrckova, F., C. De Virgilio, E. Manser, J. R. Pringle, and K. Nasmyth.** 1995. Ste20-like protein kinases are required for normal localization of cell growth and for cytokinesis in budding yeast. Genes Dev. **9:**1817–1830.
15. **DeMarini, D. J., A. E. Adams, H. Fares, C. De Virgilio, G. Valle, J. S. Chuang, and J. R. Pringle.** 1997. A septin-based hierarchy of proteins required for localized deposition of chitin in the *Saccharomyces cerevisiae* cell wall. J. Cell Biol. **139:**75–93.
16. **De Virgilio, C., D. J. DeMarini, and J. R. Pringle.** 1996. *SPR28*, a sixth member of the septin gene family in *Saccharomyces cerevisiae* that is expressed specifically in sporulating cells. Microbiology **142:**2897–2905.
17. **Dobbelaere, J., and Y. Barral.** 2004. Spatial coordination of cytokinetic events by compartmentalization of the cell cortex. Science **305:**393–396.
18. **Fares, H., L. Goetsch, and J. R. Pringle.** 1996. Identification of a developmentally regulated septin and involvement of the septins in spore formation in *Saccharomyces cerevisiae*. J. Cell Biol. **132:**399–411.
19. **Farkasovsky, M., P. Herter, B. Voss, and A. Wittinghofer.** 2005. Nucleotide binding and filament assembly of recombinant yeast septin complexes. Biol. Chem. **386:**643–656.
20. **Faty, M., M. Fink, and Y. Barral.** 2002. Septins: a ring to part mother and daughter. Curr. Genet. **41:**123–131.
21. **Field, C. M., O. Al-Awar, J. Rosenblatt, M. L. Wong, B. Alberts, and T. J. Mitchison.** 1996. A purified *Drosophila* septin complex forms filaments and exhibits GTPase activity. J. Cell Biol. **133:**605–616.
22. **Frazier, J. A., M. L. Wong, M. S. Longtine, J. R. Pringle, M. Mann, T. J. Mitchison, and C. Field.** 1998. Polymerization of purified yeast septins: evidence that organized filament arrays may not be required for septin function. J. Cell Biol. **143:**737–749.
23. **Garcia, W., A. P. de Araujo, O. Neto Mde, M. R. Ballestero, I. Polikarpov, M. Tanaka, T. Tanaka, and R. C. Garratt.** 2006. Dissection of a human septin: definition and characterization of distinct domains within human SEPT4. Biochemistry **45:**13918–13931.
24. **Gietz, R. D., and A. Sugino.** 1988. New yeast-*Escherichia coli* shuttle vectors constructed with *in vitro* mutagenized yeast genes lacking six-base pair restriction sites. Gene **74:**527–534.
25. **Gladfelter, A., L. Kozubowski, T. R. Zyla, and D. J. Lew.** 2005. Interplay between septin organization, cell cycle and cell shape in yeast. J. Cell Sci. **118:**1617–1628.
26. **Gladfelter, A. S., I. Bose, T. R. Zyla, E. S. G. Bardes, and D. J. Lew.** 2002. Septin ring assembly involves cycles of GTP loading and hydrolysis by Cdc42p. J. Cell Biol. **156:**315–326.
27. **Gladfelter, A. S., and C. Montagna.** 2007. Seeking truth on Monte Verita. Workshop on The Molecular Biology and Biochemistry of Septins and Septin Function. EMBO Rep. **8:**1120–1126.
28. **Gladfelter, A. S., J. R. Pringle, and D. J. Lew.** 2001. The septin cortex at the yeast mother-bud neck. Curr. Opin. Microbiol. **4:**681–689.
29. **Gonzalez, M. E., E. A. Peterson, L. M. Privette, J. L. Loffreda-Wren, L. M. Kalikin, and E. M. Petty.** 2007. High SEPT9_v1 expression in human breast cancer cells is associated with oncogenic phenotypes. Cancer Res. **67:**8554–8864.
30. **Gottfried, Y., A. Rotem, R. Lotan, H. Steller, and S. Larisch.** 2004. The mitochondrial ARTS protein promotes apoptosis through targeting XIAP. EMBO J. **23:**1627–1635.
31. **Guthrie, C., and G. R. Fink (ed.).** 1991. Guide to yeast genetics and molecular biology, vol. 194. Academic Press, San Diego, CA.
32. **Hall, P., and S. Russell.** 2004. The pathobiology of the septin gene family. J. Pathol. **204:**489–505.
33. **Hanrahan, J., and M. Snyder.** 2003. Cytoskeletal activation of a checkpoint kinase. Mol. Cell **12:**663–673.
34. **Harkins, H. A., N. Page, L. R. Schenkman, C. De Virgilio, S. Shaw, H. Bussey, and J. R. Pringle.** 2001. Bud8p and Bud9p, proteins that may mark the sites for bipolar budding in yeast. Mol. Biol. Cell **12:**2497–2518.
35. **Hartman, J. J., and R. D. Vale.** 1999. Microtubule disassembly by ATP-dependent oligomerization of the AAA enzyme katanin. Science **286:**782–785.
36. **Hartwell, L. H.** 1971. Genetic control of the cell division cycle in yeast. IV. Genes controlling bud emergence and cytokinesis. Exp. Cell. Res. **69:**265–276.
37. **Huang, Y. W., M. C. Surka, D. Reynaud, C. Pace-Asciak, and W. S. Trimble.** 2006. GTP binding and hydrolysis kinetics of human septin 2. FEBS J. **273:**3248–3260.
38. **Humphrey, W., A. Dalke, and K. Schulten.** 1996. VMD: visual molecular dynamics. J. Mol. Graph. **14:**33–38.
39. **Ihara, M., N. Yamasaki, A. Hagiwara, A. Tanigaki, A. Kitano, R. Hikawa, H. Tomimoto, M. Noda, M. Takanashi, H. Mori, N. Hattori, T. Miyakawa, and M. Kinoshita.** 2007. Sept4, a component of presynaptic scaffold and Lewy bodies, is required for the suppression of alpha-synuclein neurotoxicity. Neuron **53:**519–533.
40. **Iwase, M., J. Luo, E. Bi, and A. Toh-e.** 2007. Shs1 plays seperable roles in septin organization and cytokinesis in *Saccharomyces cerevisiae*. Genetics **177:**215–229.
41. **Iwase, M., J. Luo, S. Nagaraj, M. Longtine, H. B. Kim, B. K. Haarer, C. Caruso, Z. Tong, J. R. Pringle, and E. Bi.** 2006. Role of a Cdc42p effector pathway in recruitment of the yeast septins to the presumptive bud site. Mol. Biol. Cell **17:**1110–1125.
42. **John, C. M., R. K. Hite, C. S. Weirich, D. J. Fitzgerald, H. Jawhari, M. Faty, D. Schlapfer, R. Kroschewski, F. K. Winkler, T. Walz, Y. Barral, and M. O. Steinmetz.** 2007. The *Caenorhabditis elegans* septin complex is nonpolar. EMBO J. **26:**3296–3307.
43. **Joo, E., M. C. Surka, and W. S. Trimble.** 2007. Mammalian SEPT2 is required for scaffolding nonmuscle myosin II and its kinases. Dev. Cell **13:**667–690.
44. **Joo, E., C. W. Tsang, and W. S. Trimble.** 2005. Septins: traffic control at the cytokinesis intersection. Traffic **6:**626–634.
45. **Kadota, J., T. Yamamoto, S. Yoshiuchi, E. Bi, and K. Tanaka.** 2004. Septin ring assembly requires concerted action of polarisome components, a PAK Kinase Cla4p, and the actin cytoskeleton in *Saccharomyces cerevisiae*. Mol. Biol. Cell **15:**5329–5345.
46. **Keaton, M. A., and D. J. Lew.** 2006. Eavesdropping on the cytoskeleton: progress and controversy in the yeast morphogenesis checkpoint. Curr. Opin. Microbiol. **9:**540–546.

47. **Kim, H. B., B. K. Haarer, and J. R. Pringle.** 1991. Cellular morphogenesis in the *Saccharomyces cerevisiae* cell cycle: localization of the *CDC3* gene product and the timing of events at the budding site. J. Cell Biol. **112:**535–544.
48. **Kinoshita, M.** 2006. Diversity of septin scaffolds. Curr. Opin. Cell Biol. **18:**54–60.
49. **Kinoshita, M., C. M. Field, M. L. Coughlin, A. F. Straight, and T. J. Mitchison.** 2002. Self- and actin-templated assembly of mammalian septins. Dev. Cell **3:**791–802.
50. **Kinoshita, N., K. Kimura, N. Matsumoto, M. Watanabe, M. Fukaya, and C. Ide.** 2004. Mammalian septin Sept2 modulates the activity of GLAST, a glutamate transporter in astrocytes. Genes Cells **9:**1–14.
51. **Kissel, H., M. M. Georgescu, S. Larisch, K. Manova, G. R. Hunnicutt, and H. Steller.** 2005. The Sept4 septin locus is required for sperm terminal differentiation in mice. Dev. Cell **8:**353–364.
52. **Kuhlenbaumer, G., M. C. Hannibal, E. Nellis, A. Schirmacher, N. Verpoorten, J. Meuleman, G. D. Watts, E. De Vriendt, P. Young et al.** 2005. Mutations in SEPT9 cause hereditary neuralgic amytrophy. Nat. Genet. **37:**1044–1046.
53. **Lee, P. R., S. Song, H. S. Ro, C. J. Park, J. Lippincott, R. Li, J. R. Pringle, C. De Virgilio, M. S. Longtine, and K. S. Lee.** 2002. Bni5p, a septin-interacting protein, is required for normal septin function and cytokinesis in *Saccharomyces cerevisiae*. Mol. Cell. Biol. **22:**6906–6920.
54. **Lindsey, R., and M. Momany.** 2006. Septin localization across kingdoms: three themes with variations. Curr. Opin. Microbiol. **9:**559–565.
55. **Longtine, M. S., and E. Bi.** 2003. Regulation of septin organization and function in yeast. Trends Cell Biol. **13:**403–409.
56. **Longtine, M. S., H. Fares, and J. R. Pringle.** 1998. Role of the yeast Gin4p protein kinase in septin assembly and the relationship between septin assembly and septin function. J. Cell Biol. **143:**719–736.
57. **Longtine, M. S., A. I. McKenzie, D. J. Demarini, N. G. Shah, A. Wach, A. Brachat, P. Philippsen, and J. R. Pringle.** 1998. Additional modules for versatile and economical PCR-based gene deletion and modification in *Saccharomyces cerevisiae*. Yeast **14:**953–961.
58. **Longtine, M. S., C. L. Theesfeld, J. N. McMillan, E. Weaver, J. R. Pringle, and D. J. Lew.** 2000. Septin-dependent assembly of a cell cycle-regulatory module in *Saccharomyces cerevisiae*. Mol. Cell. Biol. **20:**4049–4061.
59. **Marks, B., M. H. Stowell, Y. Vallis, I. G. Mills, A. Gibson, C. R. Hopkins, and H. T. McMahon.** 2001. GTPase activity of dynamin and resulting conformation change are essential for endocytosis. Nature **410:**231–235.
60. **Martinez, C., M. Sanjuan, J. Dent., L. Karlsson, and J. Ware.** 2004. Human septin-septin interactions as a prerequisite for targeting septin complexes in the cytosol. Biochem. J. **382:**783–791.
61. **Marti-Renom, M. A., A. C. Stuart, A. Fiser, R. Sanchez, F. Melo, and A. Sali.** 2000. Comparative protein structure modeling of genes and genomes. Annu. Rev. Biophys. Biomol. Struct. **29:**291–325.
62. **Mendoza, M., A. A. Hyman, and M. Glotzer.** 2002. GTP binding induces filament assembly of a recombinant septin. Curr. Biol. **12:**1858–1863.
63. **Pan, F., R. L. Malmberg, and M. Momany.** 2007. Analysis of septins across kingdoms reveals orthology and new motifs. BMC Evol. Biol. **7:**103.
64. **Park, H. O., and E. Bi.** 2007. Central roles of small GTPases in the development of cell polarity in yeast and beyond. Microbiol. Mol. Biol. Rev. **71:**48–96.
65. **Pringle, J. R., A. E. Adams, D. G. Drubin, and B. K. Haarer.** 1991. Immunofluorescence methods for yeast. Methods Enzymol. **194:**565–602.
66. **Schenkman, L. R., C. Caruso, N. Page, and J. R. Pringle.** 2002. The role of cell cycle-regulated expression in the localization of spatial landmark proteins in yeast. J. Cell Biol. **156:**829–841.
67. **Schmidt, M., A. Varna, T. Drgon, B. Bowers, and E. Cabib.** 2003. Septins, under Cla4p regulation, and the chitin ring are required for neck integrity in budding yeast. Mol. Biol. Cell **14:**2128–2141.
68. **Sheff, M. A., K. S. Thorn, and A. Gabriel.** 2004. Optimized cassettes for fluorescent protein tagging in *Saccharomyces cerevisiae*. Yeast **21:**661–670.
69. **Sheffield, P. J., C. J. Oliver, B. E. Kremer, S. Sheng, Z. Shao, and I. G. Macara.** 2003. Borg/septin interactions and the assembly of mammalian septin heterodimers, trimers and filaments. J. Biol. Chem. **278:**3483–3488.
70. **Sirajuddin, M., M. Farkasovsky, F. Hauer, D. Kuhlmann, I. G. Macara, M. Weyand, H. Stark, and A. Wittinghofer.** 2007. Structural insight into filament formation by mammalian septins. Nature **449:**311–315.
71. **Smolka, M. B., S. H. Chen, P. S. Maddox, J. M. Enserink, C. P. Albuquerque, X. X. Wei, A. Desai, R. D. Kolodner, and H. Zhou.** 2006. An FHA domain-mediated protein interaction network of Rad53 reveals its role in polarized cell growth. J. Cell Biol. **175:**743–753.
72. **Spiliotis, E. T., and W. J. Nelson.** 2006. Here come the septins: novel polymers that coordinate intracellular functions and organization. J. Cell Sci. **119:**4–10.
73. **Sprang, S. R.** 1997. G protein mechanisms: insights from structural analysis. Annu. Rev. Biochem. **66:**639–678.
74. **Versele, M., B. Gullbrand, M. J. Shulewitz, V. J. Cid, S. Bahmanyar, R. E. Chen, P. Barth, T. Alber, and J. Thorner.** 2004. Protein-protein interactions governing septin heteropentamer assembly and septin filament 0rganization in *Saccharomyces cerevisiae*. Mol. Biol. Cell **15:**4568–4583.
75. **Versele, M., and J. Thorner.** 2004. Septin collar formation in budding yeast requires GTP binding and direct phosphorylation by the PAK, Cla4. J. Cell Biol. **164:**701–715.
76. **Vrabioiu, A. M., S. A. Gerber, S. P. Gygi, C. M. Field, and T. J. Mitchison.** 2004. The majority of the *S. cerevisiae* septin complexes do not exchange guanine nucleotide. J. Biol. Chem. **279:**3111–3118.
77. **Vrabioiu, A. M., and T. J. Mitchison.** 2006. Structural insights into yeast septin organization from polarized fluorescence microscopy. Nature **443:** 466–469.
78. **Zervos, A. S., J. Gyuris, and R. Brent.** 1993. Mxi1, a protein that specifically interacts with Max to bind Myc-Max recognition sites. Cell **72:**223–232.